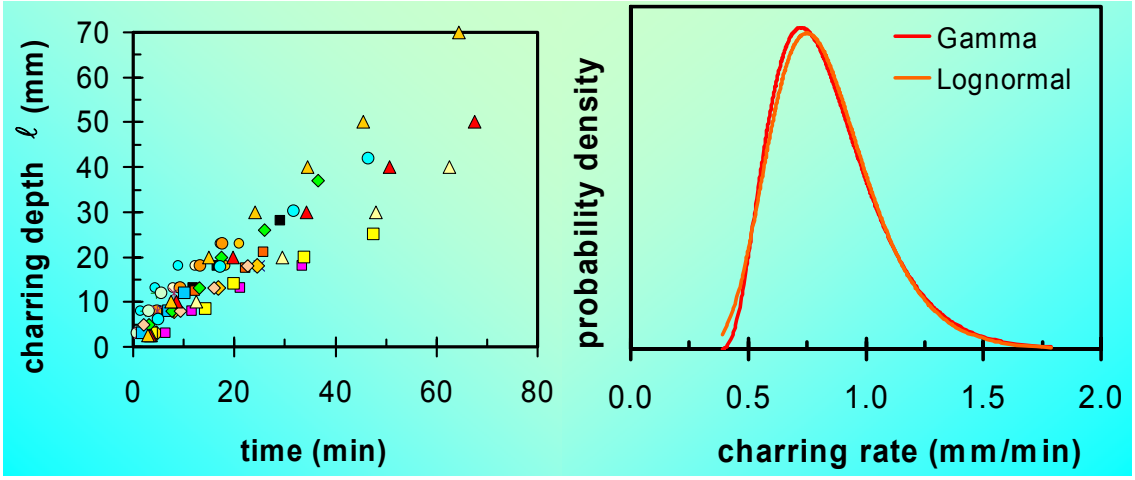

A Probabilistic Approach to Wood Charring Rate

Jukka Hietaniemi
VTT Building and Transport

ISBN 951–38–6583–5 (URL: http://www.vtt.fi/inf/pdf/)
ISSN 1459–7683 (URL: http://www.vtt.fi/inf/pdf/)

JULKAISIJA – UTGIVARE – PUBLISHER

VTT, Vuorimiehentie 5, PL 2000, 02044 VTT
puh. vaihde 020 722 111, faksi 020 722 4374

VTT, Bergsmansvägen 5, PB 2000, 02044 VTT
tel. växel 020 722 111, fax 020 722 4374

VTT Technical Research Centre of Finland, Vuorimiehentie 5, P.O.Box 2000, FI–02044 VTT, Finland
phone internat. +358 20 722 111, fax +358 20 722 4374

VTT Rakennus- ja yhdyskuntatekniikka, Kivimiehentie 4, PL 1803, 02044 VTT
puh. vaihde 020 722 111, faksi 020 722 4815

VTT Bygg och transport, Stenkarlsvägen 4, PB 1803, 02044 VTT
tel. växel 020 722 111, fax 020 722 4815

VTT Building and Transport, Kivimiehentie 4, P.O.Box 1803, FI–02044 VTT, Finland
phone internat. +358 20 722 111, fax +358 20 722 4815

Technical editing Maini Manninen

Published by

Series title, number and report code of publication

VTT Working Papers 31
VTT–WORK–31

Author(s)
Hietaniemi, Jukka

Title

A Probabilistic Approach to Wood Charring Rate

Abstract

This report presents a probabilistic model for wood charring rate and an application of the model to assess fire resistance of a wooden load-bearing beam. The model is an empical one, based on quantification of the dependence of the wood charring rate on the principal physical factors governing the charring process. These factors include the influence of the heat flux exposing the wood surface, the wood density and moisture content as well as the ambient oxygen concentration. The application introduces a novel approach to assess the endurance of a wooden structural member in a natural fire conditions, which uses probabilistic fire simulation to quantify the heat exposure and the char depth of the structural member. The principal result of the approach is the time evolution of the conditional failure probability of failure of the structural wooden member, which can be further elaborated by incorporating into the analysis the statistical and modelling results determining the frequency of the conditioning factor, *i.e.*, the occurrence of a fire with sufficient severity to potentially compromise the structural safety.

Keywords
construction materials, wood charring, charring rate, charring depth, probabilistic methods, Monte Carlo, fire resistance, beams, glulam, fire simulation, cone calorimeters, standards, ISO 834

Activity unit
VTT Building and Transport, Kivimiehentie 4, P.O.Box 1803, FI–02044 VTT, Finland

ISBN		Project number
951–38–6583–5 (URL: http://www.vtt.fi/inf/pdf/)		R4SU00235
Date July 2005	Language English	Pages 53 p.
Name of project New simulation methods for fire safety analysis	Commissioned by Tekes & VTT	
Series title and ISSN VTT Working Papers 1459–7683 (URL: http://www.vtt.fi/inf/pdf/)	Publisher VTT Information Service P.O. Box 2000, FI–02044 VTT, Finland Phone internat. +358 20 722 4404 Fax +358 20 722 4374	

Preface

Charring rate is the basic quantity of assessment of fire resistance of wooden structural members. Due to the inherent variabilities and uncertainties involved in the fire exposure and the charring process, the charring rate is factor with substantial uncertainty which should be taken into account in any assessment of fire resistance of wooden members, in particular in the probabilistic approaches to assess fire resistance. This report presents a probabilistic model for wood charring rate based on quantification of the dependence of the wood charring rate on the principal physical factors governing the charring process as well as an application of the model to assess in a probabilistic manner the fire resistance of wooden beam.

The work has been out in the Fire Research group of VTT Building and Transport, Finland. It forms a part of a larger research project launched to develop new tools for fire simulation with the aim set at producing generally acceptable and valid science-based tools to meet the needs of fire safety design and risk assessment within the industry and other stakeholders.

The project is funded by the National Technology Agency of Finland (Tekes) and VTT Building and Transport.

Contents

1. Introduction

This report presents a probabilistic model for wood charring rate and an application of the model to assess fire resistance of a wooden load-bearing beam. The model is an empical one, based on quantification of the dependence of the wood charring rate on the principal physical factors governing the charring process. These factors include the influence of the heat flux exposing the wood surface, the wood density and moisture content as well as the ambient oxygen concentration. The application introduces a novel approach to assess the endurance of a wooden structural member in a natural fire conditions, which uses probabilistic fire simulation to quantify the heat exposure and the char depth of the structural member. The principal result of the approach is the time evolution of the conditional failure probability of failure of the structural wooden member, which can be further elaborated by incorporating into the analysis the statistical and modelling results determining the frequency of the conditioning factor, *i.e.*, the occurrence of a fire with sufficient severity to potentially compromise the structural safety.

2. Development of the model

In this Chapter we derive an analytical expression for the wood charring rate and quantify its uncertainty. The presentation is based on the approach of Mikkola (1990) who studied the dependence of the wood charring rate

$$\beta = \frac{dx_{char}}{dt} \tag{1}$$

where x_{char} is the position of the char front and t is time on the following factors:

- wood density ρ,
- wood moisture content w,
- external heat flux $\dot{q}''_e$,
- oxygen content χ_{O2}.

Below, in section 2.1 we present a new analysis of the influence of these factors on the wood charring rate. Besides the four factors listed above, also the char layer thickness has a significant influence on the wood charring: charring is considerably slower beneath a thick char layer than a thin one. The influence of the char layer thickness on the wood charring rate is analysed in section 2.2 on the basis of the time-dependence of the char-layer depth and the charring rate.

2.1 Influence of density, external heat flux, moisture contents and oxygen concentration

By applying a simple energy-balance consideration to the charring front, Mikkola (1990) equates the heat flux entering to the charring front $\dot{q}''_n$ to the energy per unit area required to heat up to the wood from its initial temperature T_0 to the pyrolysis temperature T_p as well as to pyrolyse the wood which requires energy an amount of L_v:

$$\dot{q}''_n = \dot{q}''_e - \dot{q}''_L - \dot{q}''_c = \dot{m}''\left[C\left(T_p - T_0\right) + L_v\right] \tag{2}$$

where $\dot{m}''$ is the mass flow per unit area of the pyrolysis products (mass flux units of $kgm^{-2}s^{-1}$), $\dot{q}''_L$ describes the heat losses at the sample surface, $\dot{q}''_c$ is the energy flux absorbed by the char and C is the specific heat of the wood.

In the conditions of complete combustion the mass flux of the pyrolysates equals the mass loss rate per unit area of the sample and, further, as the mass loss rate can be expressed in terms of the wood density and the charring rate as

$$\dot{m}'' = \rho\beta\,, \tag{3}$$

one gets the following relation between the charring rate β and the external heat flux $\dot{q}_e''$ and the wood density ρ:

$$\beta = \frac{\dot{q}_e'' - \dot{q}_L'' - \dot{q}_c''}{\rho\left[C\left(T_p - T_0\right) + L_v\right]} \approx \frac{\dot{q}_e'' - \dot{q}_L''}{\rho\left[C\left(T_p - T_0\right) + L_v\right]}, \tag{4}$$

where the second approximate equality follows from the fact that the in the conditions corresponding to the fire environments, the energy absorbed by the char $\dot{q}_c''$ is small as compared to other terms.

The equation given above gives a simple description of the influence of the most important factors on the charring rate of wood. We use it as a starting for refinements explained below.

2.1.1 Density dependence

Mikkola (1990) points out that the density dependence of the charring rate is not simple inverse proportionality, but rather of a form

$$\beta \propto \left(\rho + \rho_0\right)^{-1}, \tag{5}$$

where ρ_0 is a parameter that can be determined on the basis of experimental findings. On the basis of the results of Schaffer (1967), Mikkola (1990) suggest that ρ_0 = 120 kg/m^3. We, however, propose a different value: ρ_0 = 465 kg/m^3 ± 40 % (the variability can be interpreted as 95 % confidence interval), *i.e.*,

$$\beta \approx \frac{\dot{q}_e'' - \dot{q}_L''}{\left(\rho + \rho_0\right)\left[C\left(T_p - T_0\right) + L_v\right]}, \tag{6}$$

where we can assume that the parameter ρ_0 is a normally distributed quantity with mean equal to m_ρ = 465 kg/m^3 and standard deviation equal to s_ρ = 90 kg/m^3 or formally:

$$\rho_0 \propto N\left(465;93\right)\mathrm{kgm}^{-3}, \tag{7}$$

where $N(m_\rho;s_\rho)$ denotes the normal distribution. This value of ρ_0 is based on analysis of data of Tran & White (1992) and Njankouo *et al*. (2004) for wood samples with moisture of about 8–10 %, see Figure 1.

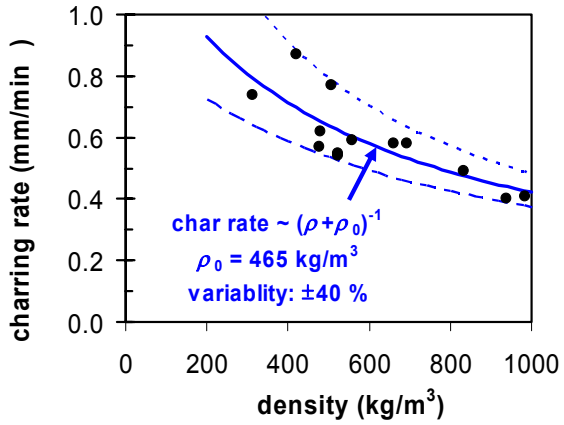

Figure 1. Dependence on wood charring rate on the density according to data of Tran & White (1992) and Njankouo et al. (2004).

2.1.2 Moisture content dependence

To elucidate the dependence of the charring rate on the moisture content of the wood, Mikkola (1990) analyses the moisture dependence of the wood specific heat arriving at the expression

$$C(T_p - T_0) = C_1(T_v - T_0) + C_2(T_p - T_v) + (C_w - C_1)(T_v - T_0)\cdot w, \tag{8}$$

where the w is the moisture of the wood defined as

$$w = \frac{m - m_0}{m_0}, \tag{9}$$

where m is the mass of the (moist) sample and m_0 is the mass of the sample with no water in it (*e.g.*, dried in oven above 100 °C). The temperature rise from T_0 to T_p is broken here to two parts, one part taking place below the water vaporisation temperature T_v (≈ 100 °C), characterised by specific heat C_1 and the other part taking place between the water vaporisation temperature T_v and T_p with specific heat equal to C_2. Using the specific heat data shown in Figure 2, we may write

$$C(T_p - T_0) = a + b\cdot w, \tag{10}$$

where

$$\begin{cases} a = 502\ (140)\ \text{kJ/kg} \\ b = 226\ (34)\ \text{kJ/kg} \end{cases}, \tag{11}$$

where the numbers in the parentheses express the standard deviation associated with the value of the parameter.

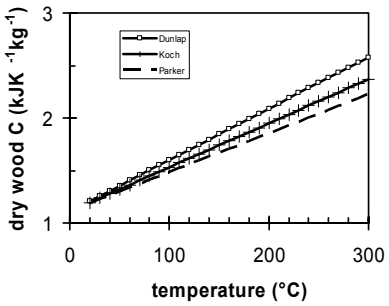

Figure 2. Dependence of the specific heat of dry wood on temperature according to Dunlap (1912), Koch (1969) and Parker (1985).

The heat of vaporisation includes contributions of the heat of vaporisation of dry wood $L_{v,0}$ and water

$$L_v = L_{v,0} + L_w \cdot w, \tag{12}$$

where $L_w = 2260$ kJ/kg is the heat of vaporisation of water. The values of the heat of vaporisation of dry wood given in literature vary considerably: e.g. Mikkola (1989, p. 30) quotes a value of 2250 kJ/kg while one may find as low values as 300 kJ/kg (de Souza Costa & Sandberg 2004). The large scatter in the reported values reflects the fact that actually the heat of vaporisation of dry wood is not constant during the process of wood pyrolysis, *e.g.*, Tinney (1965) reports that "before a break point", $L_{v,0} = 125$–210 kJ/kg and "after a break point", $L_{v,0} = 840$–2300 kJ/kg. As it is very difficult to select the "proper" value for $L_{v,0}$ we proceed to assess a value suitable for the present context by analysis of data presented by Mikkola (1990, p. 24, Fig. 4) which presents the relative charring rate as a function of the wood moisture. For this analysed we write

$$\frac{\beta}{\beta_{ref}} = \frac{a_1}{a + L_{v,0} + (b + L_w) \cdot w}, \tag{13}$$

and use least-squares curve fitting to establish the unknown quantity $L_{v,0}$ as well as the auxiliary parameter a_1 (note that here, the dimensions of the variables are kJ/kg). The least-squares analysis augmented by an uncertainty assessment (see Figure 3) gives a result

$$L_{v,0} \approx 300\,(100)\,\text{kJ/kg}. \tag{14}$$

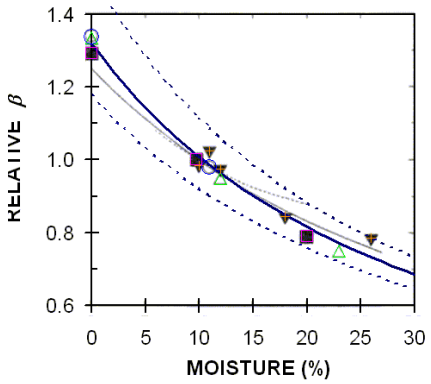

Figure 3. Dependence of the wood charring rate on the wood moisture (Mikkola 1990 and refs. ib id). The thick curve is a least-squares fitting results yielding $L_{v,0}$ = 300 (100) kJ/kg where there uncertainty interval has been assessed so that the calculated curves (the dotted curves) make an envelope to the data values.

The analysis presented above allows us to write the dependence of the wood charring rate on external heat flux $\dot{q}''_e$, wood density ρ and wood moisture content w as

$$\beta \approx \frac{\dot{q}''_e - \dot{q}''_L}{(\rho + \rho_0)(A + B \cdot w)}, \tag{15}$$

where[1]

$$\begin{cases} A = 502\,(140)\ \text{kJ/kg} + 300(100)\ \text{kJ/kg} = 800\,(170)\ \text{kJ/kg} \\ B = 226\,(34)\ \text{kJ/kg} + 2260\ \text{kJ/kg} = 2490\,(34)\ \text{kJ/kg} \end{cases}, \tag{16}$$

or, assuming that A and B are uniformly distributed quantities with mean values of 800 kJ/kg and 2490 kj/kg and standard deviations of 170 kJ/kg and 34 kJ/kg, we can write

$$\begin{cases} A \propto U(505;1095)\ \text{kJ/kg} \\ B \propto U(2430;2550)\ \text{kJ/kg} \end{cases}, \tag{17}$$

where $U(x_{min}, x_{max})$ symbolises the uniform distribution between x_{min} and x_{max}.

[1] Here we assume that the uncertainty of the water heat of vaporisation is much smaller than the uncertainties of the other quantities.

2.1.3 External radiation dependence

The dependence of the heat losses on the external radiation may be assessed via the surface temperature T_s, as the loss term may be expressed as

$$\dot{q}''_L \approx h_s \cdot (T_s - T_\infty) + \varepsilon_s \cdot \sigma \cdot T_s^4 \,\mathrm{kW/m^2}, \tag{18}$$

where T_∞ is the ambient temperature (assumed to be 20 °C), ε_s is the surface emissivity and h_s is the heat transfer coefficient on the surface and $\sigma = 5{,}67 \cdot 10^{-8}$ $\mathrm{WK^{-4}m^{-2}}$ is the Stefan-Boltzman constant.

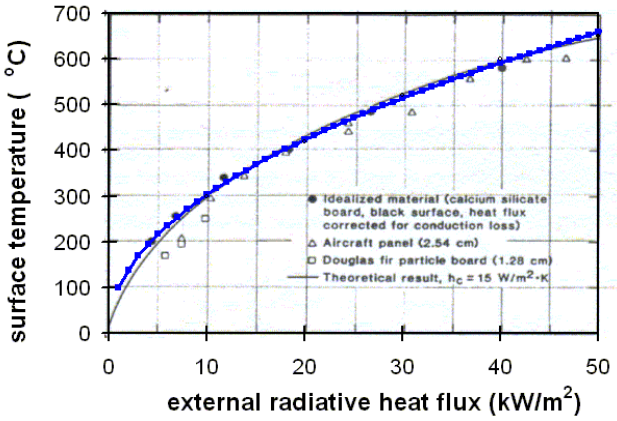

Figure 4. Dependence of the surface temperature on the external radiative heat flux (Quintiere & Harkleroad 1985). A simple power-law fit is presented by the thick blue curve.

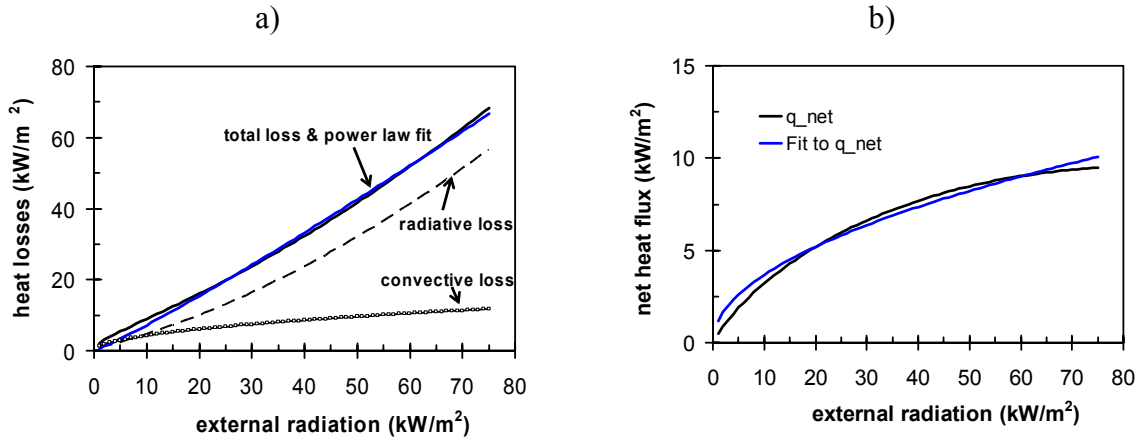

Figure 5. a) Heat losses calculated on the basis of the surface temperature. b) Dependence of the net heat flux on the external radiative heat flux and a simple a simple power-law fit.

The two heat transfer parameters, ε_s and hs, are not know with high accuracy. Our approach to assigning values to them is giving ε_s a fixed value of 0,75 and letting h_s vary between 11 $\mathrm{WK^{-1}m^{-2}}$ and 15 $\mathrm{WK^{-1}m^{-2}}$ according to a triangular distribution peaked at 13,5 11 $\mathrm{WK^{-1}m^{-2}}$. In the conditions relevant to fire applications, the heat losses from the surface are mainly due to radiative losses, the second term but convective portion (the first term) is not negligible, though as thus we retain it in the further analysis. Quintiere and Harkleroad (1985) present a graph of the dependence of the surface temperature of the external radiative heat flux; this graph is reproduced below (Figure 4) with a simple least-squares fitted power-law curve of the form

$$T_s = 99{,}6 \cdot \left(\frac{\dot{q}''_e}{\mathrm{kW/m^2}} \right)^{0{,}483} \,^{\circ}\mathrm{C} \tag{19}$$

presented as the thick blue curve. Inserting this relation to the above formula for the heat losses, we obtain the result shown in Figure 5a with the heat loss expressed approximately as

$$\dot{q}''_L = 0{,}559 \cdot \left(\frac{\dot{q}''_e}{\mathrm{kW/m^2}} \right)^{1{,}107} \mathrm{kW/m^2}, \tag{20}$$

The net heat flux is obtained by subtracting the heat losses from the external heat flux, see Figure 5b. Using again a simple power-law description for the dependence of the net heat flux on the external heat flux, we obtain the result

$$\dot{q}''_n \approx \dot{q}''_e - \dot{q}''_L = \vartheta \cdot \left(\frac{\dot{q}''_e}{\mathrm{kW/m^2}} \right)^{p}, \tag{21}$$

where the

$$p = 0{,}5\,, \tag{22}$$

and the parameter ϑ reflects the uncertainties in the heat transfer parameters (*i.e.*, the random nature of the heat transfer coefficient h_s); also ϑ follows the triangular distribution with minimum, maximum and peak value equal to 1,026 $\mathrm{kW/m^2}$, 1,387 $\mathrm{kW/m^2}$ and 1,162 $\mathrm{kW/m^2}$, respectively, *i.e.*,

$$\vartheta \propto \Delta(1{,}026; 1{,}387; 1{,}162)\,\mathrm{kW/m^2}\,, \tag{23}$$

where Δ denotes the triangular statistical distribution (the standard deviation of thus equals 0,070 $\mathrm{kW/m^2}$). The uncertainty of the parameter p is analysed in the following.

White & Tran (1996) have studied the dependence of the charring rate of four different wood species on the external constant heat flux. The wood species and their density and moisture contents are the following:

- Redwood, $\rho = 312$ kg/m^3, $w = 8{,}3$ %;
- Basswood, $\rho = 420$ kg/m^3, $w = 8{,}1$ %;
- Southern Pine, $\rho = 508$ kg/m^3, $w = 9{,}7$ %;
- Red Oak, $\rho = 660$ kg/m^3, $w = 8{,}5$ %.

We analysed the charring rate data of White & Tran (1996) by fitting power-law curves of the form

$$\beta = a_2 \cdot \dot{q}_e''^{p}, \tag{24}$$

to the data. Two fitting approaches employed, one in which both a_2 and p were adjusted in the residual-squares minimisation (see Figure 6, the left hand-side figures) and the other in which the power p was fixed to value $p = 0{,}5$ (see Figure 6, the left hand-side figures). It may be seen from Figure 6 that the fits obtained with the fixed power of $p = 0{,}5$ are very good with no practically significant difference to the best fit obtained by tuning both a_2 and p_2.

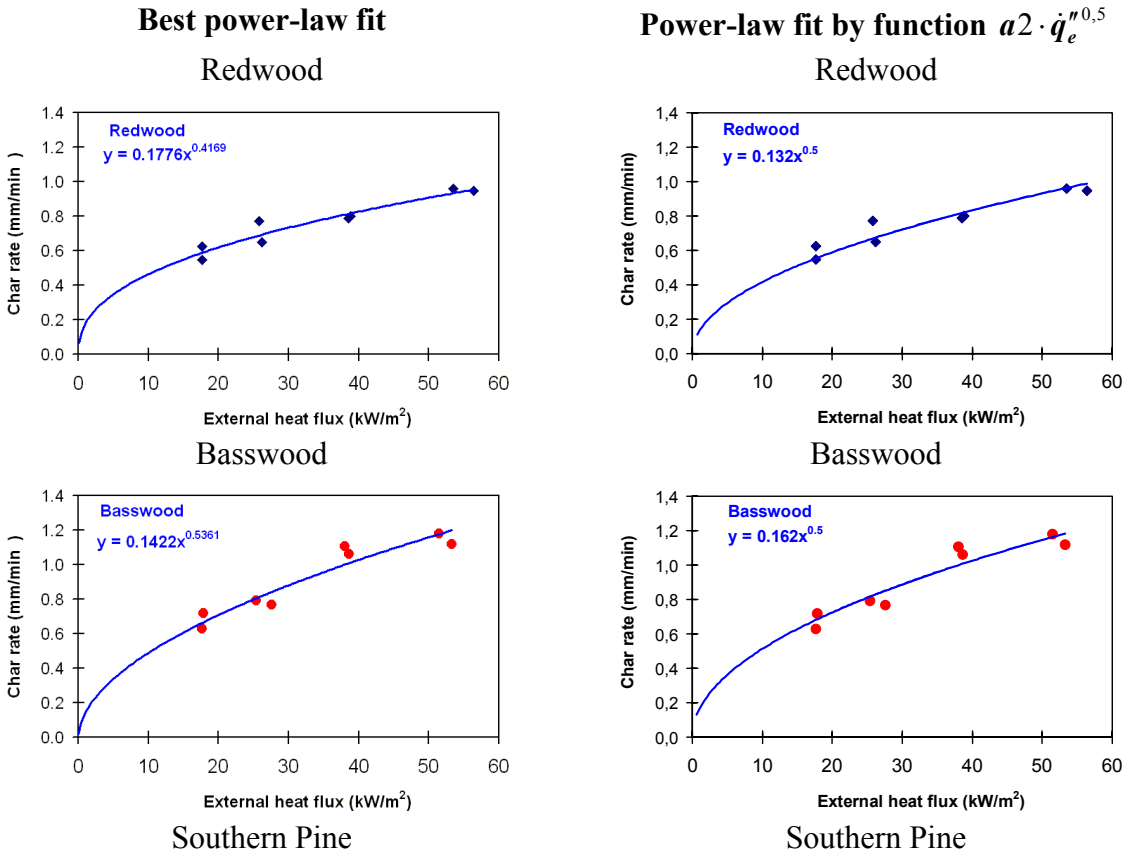

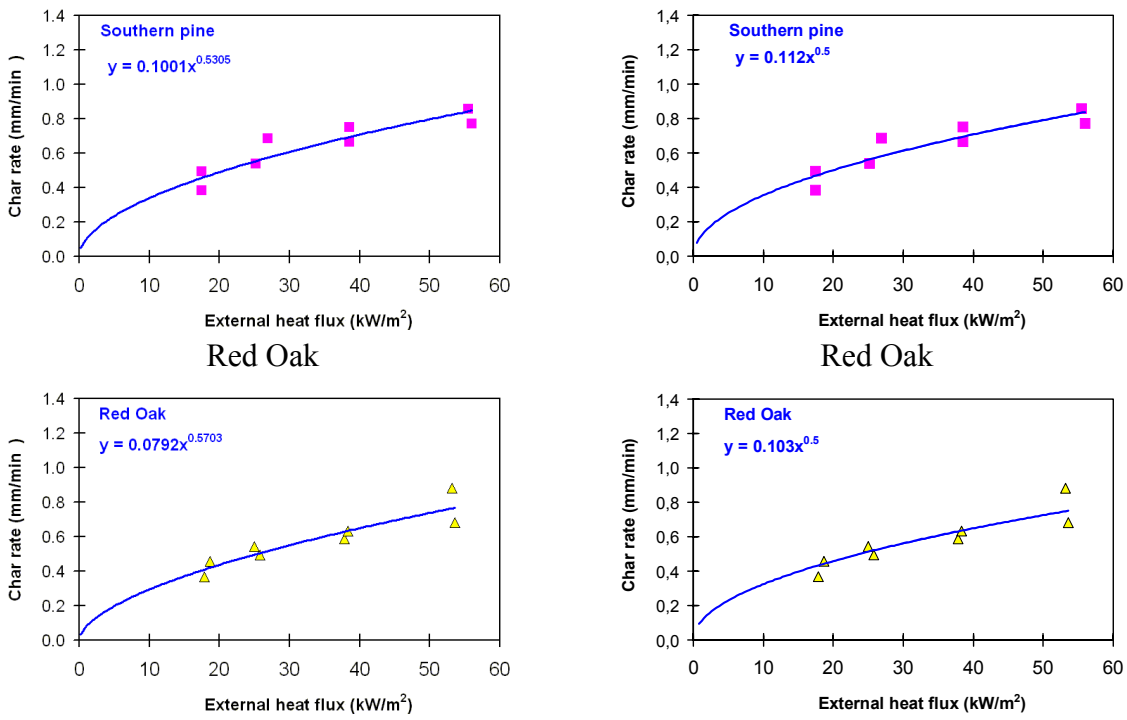

Figure 6. Analysis of the data of White & Tran (1996, Fig. 2) on the dependence of the charring rate on the external heat flux using power-law functions: on left-hand side we show the best fit and on the right-hand side fit results using a fixed power equal to 0,5.

Table 1 summarises the four estimates $p^{(k)}$, $k = 1, 2, 3, 4$, obtained from the four data sets. The final (unbiased) estimate for p and its uncertainty Δp can be obtained as uncertainty-weighted sums (Bevington & Robinson 1992):

$$p \approx \sqrt{\sum_{k=1}^{4}\left(\frac{p^{(k)}}{\Delta p^{(k)}}\right)^2 \Bigg/ \left(\frac{1}{\Delta p^{(k)}}\right)^2} = 0{,}50$$
$$\Delta p \approx \sqrt{\sum_{k=1}^{4}\left(\frac{1}{\Delta p^{(k)}}\right)^{-2}} = 0{,}04 \quad . \tag{25}$$

We may assume that a suitable distribution characterising p is the normal distribution, i.e.,

$$p \propto N(0{,}50;0{,}04) \ . \tag{26}$$

Table 1. Analysis of the parameter p and its uncertainty estimate Δp.

Species	density ρ (kg/m^3)	w %	p -	Δp -
Redwood	312	8,3	0,417	0,058
Basswood	420	8,1	0,536	0,066
Southern Pine	508	9,7	0,531	0,099
Red Oak	660	8,5	0,570	0,092
			p_{avg} =	**0,50**
			Δp_{avg} =	**0,04**

Inserting the above expression for the net heat flux to the formula of the charring rate yields

$$\beta \approx \frac{\vartheta \cdot \dot{q}_e''^p}{(\rho + \rho_0)\left[C(T_p - T_0) + L_v\right]}, \tag{27}$$

where the external heat flux $\dot{q}_e''$ is expressed in units of kW/m^2. As this expression is based on an approximate analysis, it is plausible to expect that it reproduces the functional dependence of the charring rate of the most important factors, but not that it would reproduce accurately experimentally observed value. Thus, to allow for tuning of the charring rate to match experimentally observed values, we augment the above expression by a constant factor ψ hence obtaining

$$\beta \approx \psi \frac{\vartheta \cdot \dot{q}_e''^p}{(\rho + \rho_0)\left[C(T_p - T_0) + L_v\right]}. \tag{28}$$

2.1.4 Oxygen concentration dependence

We incorporate the influence of the oxygen concentration to the wood charring rate by adding a factor $f(\chi_{O2})$ that depends on the oxygen concentration χ_{O2} to the above expression of β:

$$\beta \approx f(\chi_{O2}) \cdot \psi \cdot \frac{\vartheta \cdot \dot{q}_e''^p}{(\rho + \rho_0)(A + B \cdot w)}. \tag{29}$$

In the light of the data of Ohnemiller et al. (1987) and Nurbakhsh (1989) quoted by Mikkola (1990, p. 26), the function $f(\chi_{O2})$ has a shape shown in Figure 7. The mathematical form of this function can be expressed as

$$f(\chi_{O2}) = \xi + (1-\xi)\cdot\left(\frac{\chi_{O2}}{\chi_{O2}^{(0)}}\right)^{0,737} . \tag{30}$$

where $\chi_{O2}^{(0)} = 21\%$ and ξ is random parameter ranging from 0,5 to 0,65, or, expressed in symbolic terms

$$\xi \propto U(0{,}50;0{,}65), \tag{31}$$

where U(x_{min}, x_{max}) symbolises the uniform distribution between x_{min} and x_{max}.

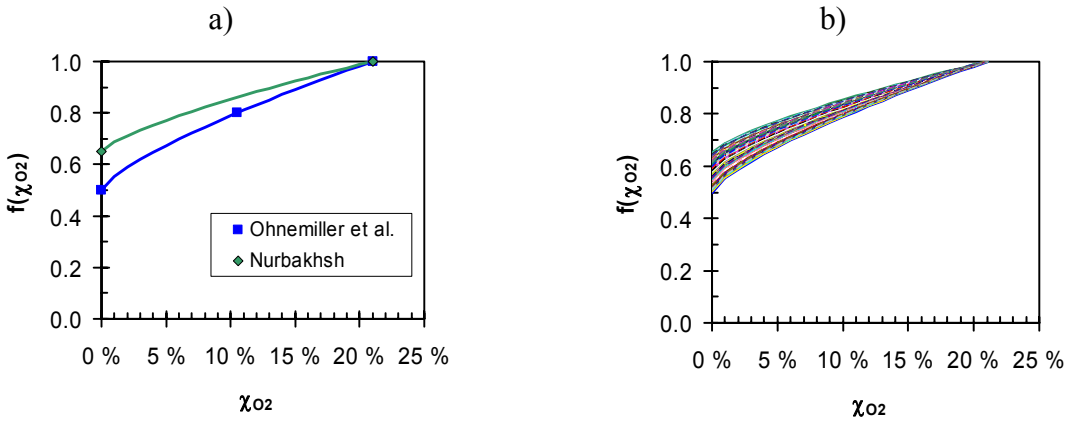

Figure 7. The function $f(\chi_{O2})$ characterising the dependence of the wood charring rate on the oxygen concentration: a) curve fitting to data of Ohnemiller et al. (1987) and Nurbakhsh (1989) and b) example describing the variability of $f(\chi_{O2})$.

Thus far we have derived the following expression for the charring rate of wood which includes explicitly the uncertainties of the influential factors:

$$\beta = f(\chi_{O2})\cdot\psi\cdot\frac{\vartheta\cdot\dot{q}_e''^{p}}{(\rho+\rho_0)(A+B\cdot w)}, \tag{32}$$

2.2 Time dependence of the char layer depth and charring rate

In this section we analyse the influence of the thickness of the char layer on the charring rate. In line with the treatise of the previous section, we continue to carry out the analysis on a phenomenological level rather than delving in details to modelling of the transfer processes involved.

2.2.1 Constant heat flux

Under constant heat flux, a first-order model for the dependence of the charring rate on the thickness ℓ of the char layer is simple exponential dependence of the form[2]

$$\ell \propto \int_0^t \psi(t')dt' = \psi_0 \cdot \tau \cdot \left[1 - \exp\left(-\frac{t}{\tau}\right)\right], \tag{33}$$

where the time constant τ and the factor ψ_0 which is of the order of unity can be determined from experimental data. Correspondingly the function $\psi(t)$ reads

$$\psi(t) = \psi_0 \cdot \exp\left(-\frac{t}{\tau}\right). \tag{34}$$

We base our determination of the function $\psi(t)$ on the data of Fredlund (1988), Tsantaridis & Östman (1998) and Mikkola (1988) shown in Figure 8.

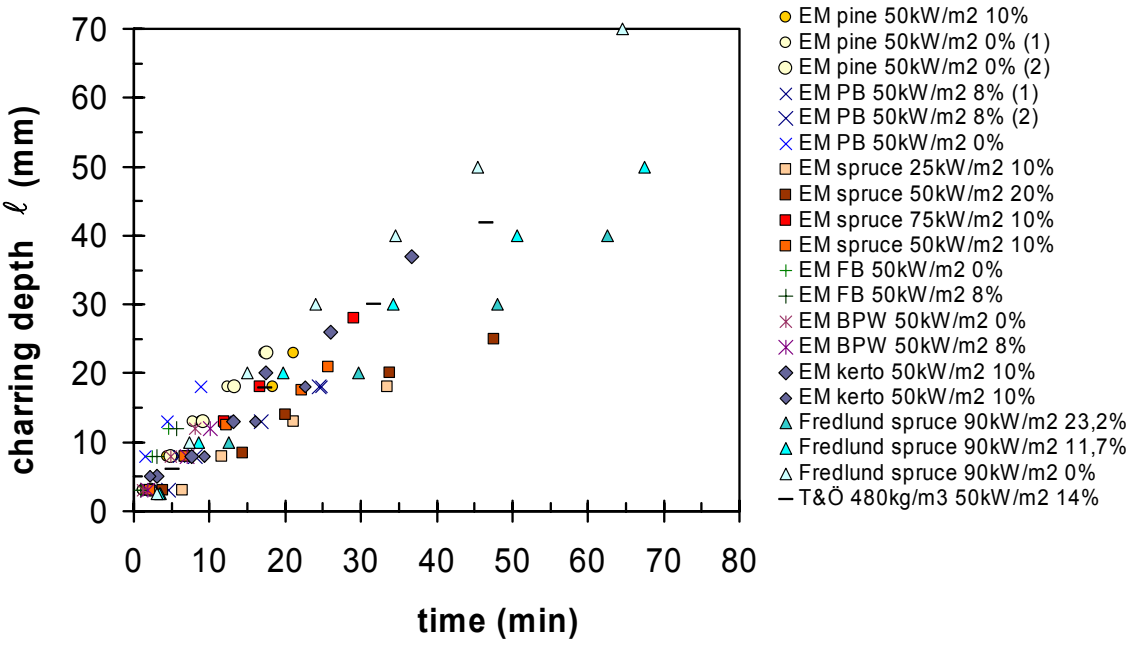

Figure 8. Data of Fredlund (1988), Tsantaridis & Östman (1998) and Mikkola (1988) on the dependence of the wood product char depth on time under constant heat flux.

[2] We add the time constant to the integral of $\psi(t)$ to keep the function $\psi(t)$ non-dimensional.

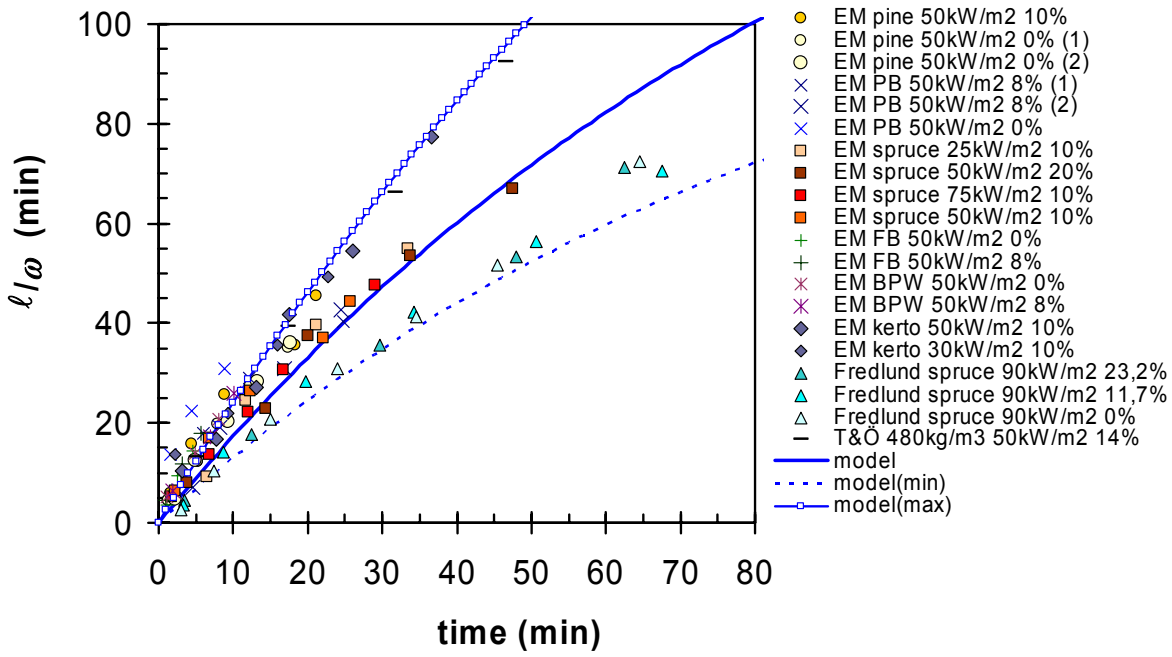

Figure 9. Analysis of data of Fredlund (1988), Tsantaridis & Östman (1998) and Mikkola (1988) on the dependence of the wood product char depth on time under constant heat flux.

By dividing the char depth data with the pre-factor depending on the heat flux, density and moisture content we obtain a empirically determined factor ℓ/ω (see Figure 9) that can be fitted by the time dependent portion of the expression of the char depth:

$$\frac{\ell}{f(\chi_{O2})\cdot\dfrac{\vartheta\cdot\dot{q}_e''^{p}}{(\rho+\rho_0)(A+B\cdot w)}}\equiv\frac{\ell}{\omega}=\psi_0\cdot\tau\left(1-\exp\left(-\frac{t}{\tau}\right)\right), \tag{35}$$

Curve fitting yields the following results for the parameter ψ_0 and τ as well as their uncertainty estimate:

$$\begin{aligned}&\psi_{0,avg}=3{,}6;\ \psi_{0,\min}=2{,}7;\ \psi_{0,\max}=5{,}0;\\&\tau_{avg}=100\,\text{min};\ \tau_{\min}=90\,\text{min};\ \tau_{\max}=110\,\text{min}\end{aligned}. \tag{36}$$

If we assume that these parameters follow that triangular distribution we may write

$$\begin{aligned}&\psi_0\propto\Delta(2{,}7;\,5{,}0;\,3{,}6)\\&\tau\propto\Delta(90\,\text{min};\,110\,\text{min};\,100\,\text{min})\end{aligned}. \tag{37}$$

The product of the two constant ϑ and ψ_0 can be expressed as a single parameter C following the triangular distribution (see Figure 10):

$$C = \psi_0 \cdot \vartheta \propto \Delta(2{,}72;\ 5{,}45;\ 3{,}93)\ \mathrm{kW/m^2}\ . \tag{38}$$

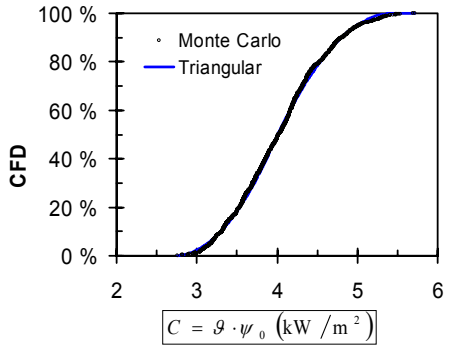

Figure 10. Monte Carlo analysis of the combination of parameters ϑ and ψ_0 to a single parameter C.

The resulting expression for the charring rate β in units of m/s is

$$\beta = f(\chi_{O2}, t) \cdot \frac{C \cdot \dot{q}''_e(t)^p}{(\rho + \rho_0)(A + B \cdot w)} \cdot \exp\left(-\frac{t}{\tau}\right), \tag{39}$$

where the model parameters are[3]

$$f(\chi_{O2}, t) = \xi + (1 - \xi) \cdot \left(\frac{\chi_{O2}(t)}{\chi_{O2}^{(0)}}\right)^{0{,}737}\ . \tag{40}$$

$$C \propto \Delta(2{,}72;\ 5{,}45;\ 3{,}93)\ \mathrm{kW/m^2}\ , \tag{41}$$

$$\rho_0 \propto N(465;93)\ \mathrm{kgm^{-3}}, \tag{42}$$

$$\begin{cases} A \propto U(505;1095)\ \mathrm{kJ/kg\ (average = 800\ kJ/kg)} \\ B \propto U(2430;2550)\ \mathrm{kJ/kg\ (average = 2490\ kJ/kg)} \end{cases}, \tag{43}$$

$$p \propto N(0{,}50;0{,}04)\ . \tag{44}$$

[3] $N(\mu;\sigma)$ is the Normal distribution with mean μ and standard deviation σ; $\Delta(x_{min};x_{max},x_{peak})$ is the triangular distribution with minimum value x_{min}, maximum value x_{max} and peak value x_{peak}; $U(x_{min};x_{max})$ is the uniform distribution with minimum value x_{min} and maximum value x_{max}.

$$\tau \propto \Delta(90;110;100)\,\text{min}. \tag{45}$$

$$\xi \propto U(0{,}50;0{,}65)\,(\text{average} = 0{,}575), \tag{46}$$

and the influential factors are

- external heat flux $\dot{q}''_e(t)$ which may depend on time *t*,
- wood density ρ,
- wood moisture content *w*,
- oxygen content $\chi_{O2}(t)$ which may depend on time *t*.

The parameter $\chi_{O2}^{(0)} = 21\%$ is the normal volumetric oxygen concentration.

2.2.2 Time dependent heat flux: the standard fire exposure

The most familiar case of time-dependent heat flux is the heating of a wooden sample in a furnace the temperature of which follows the standard curve

$$T_f(t) = T_0 + 345\,^{\circ}\text{C} \cdot \log_{10}\left(8 \cdot \left(\frac{t}{\text{min}}\right) + 1\right), \tag{47}$$

where the initial temperature T_0 is often 20 °C. A typical uncertainty related to standard fire curves produces in laboratory conditions is about ±5 %, see Figure 11. Inspection of heat flux data measured by a heat-flux gauge during heating corresponding to the standard temperature, Figure 12, reveals that before about 10 min, the heat flux $\dot{q}''_{std}(t)$ grows approximately linearly and after about 10 minutes, the heat flux can be calculated as the heat radiation with an effective emissivity equal to ε_{eff}, or

$$\dot{q}''_{std}(t) = \begin{cases} k \cdot t & t < 10\,\text{min} \\ \varepsilon_{eff} \cdot \sigma \cdot \left[T_f(t) + 273{,}15\,^{\circ}\text{C}\right]^4, & t \geq 10\,\text{min} \end{cases}, \tag{48}$$

where

$$\begin{aligned} k &= (3{,}55 \pm 0{,}45)\,\text{kW} \cdot \text{min}^{-1}/\text{m}^2 \\ \varepsilon_{eff,avg} &= 0{,}82;\ \varepsilon_{eff,\text{min}} = 0{,}70;\ \varepsilon_{eff,\text{min}} = 0{,}90 \end{aligned}, \tag{49}$$

or expressed using the triangular distribution $\Delta(x_{\text{min}};x_{\text{max}};x_{peak})$:

$$\begin{aligned} k &\propto \Delta(3{,}10;4{,}0;3{,}55)\,\text{kW} \cdot \text{min}^{-1}/\text{m}^2 \\ \varepsilon_{eff,avg} &\propto \Delta(0{,}70;0{,}90;0{,}82) \end{aligned}. \tag{50}$$

Also the oxygen concentration in a standard fire test depends on time. According Holm and Loikkanen (1981) the oxygen concentration decreases up to about 20 minutes where after it remains relative constant. The following relation gives a simple mathematical expression for such dependence:

$$\chi_{O2}(t) = \begin{cases} \Delta\chi + (21\% - \Delta\chi)\cdot \exp\left(-\dfrac{t}{\tau_{O2}}\right), & t < 20\,\text{min} \\ \Delta\chi, & t \geq 20\,\text{min} \end{cases}. \tag{51}$$

where

$$\begin{aligned} &\text{average}\,\Delta\chi = 5{,}5\,\%,\ \text{std.deviation}\,\Delta\chi = 4{,}1\,\% \\ &\tau_{eO2} = 4\,\text{min (constant)} \end{aligned}, \tag{52}$$

or expressed using the normal distribution $N(\mu;\sigma)$:

$$\Delta\chi \propto N(5{,}5\,\%;\ 4{,}1\,\%)\ . \tag{53}$$

Thus, the time dependent part of the wood charring rate in the standard fire exposure is

$$f(\chi_{O2},t)\cdot \dot{q}''_{std}(t)^{p}\cdot \exp\left(-\frac{t}{\tau}\right). \tag{54}$$

As the functions $f(\chi_{O2},t)$ and $\exp(-t/\tau)$ decrease while the function $\dot{q}''^{\,p}_{std}$ increases with time, the product of these three functions is quite constant with respect to time, see Figure 14 which shown the average value of the time dependent part of the wood charring rate: it is seen that between 5 min and 90 min, the time-dependent part of the charring rate varies between 3,3 and 4,6, or has a value of 4,0 ± 16 %. It is this constancy of the time-dependent part that explains why the charring rates observed in standard fire test conditions are more or less constant. An example of the variability of the time-dependent part of the charring rate is shown in Figure 15.

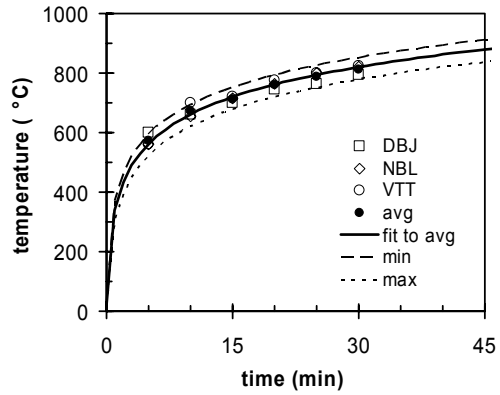

Figure 11. Standard temperature curves from three laboratories (Holm & Loikkanen 1981) (DBJ: Danish, NBL: Norwegian & VTT: Finnish laboratory).

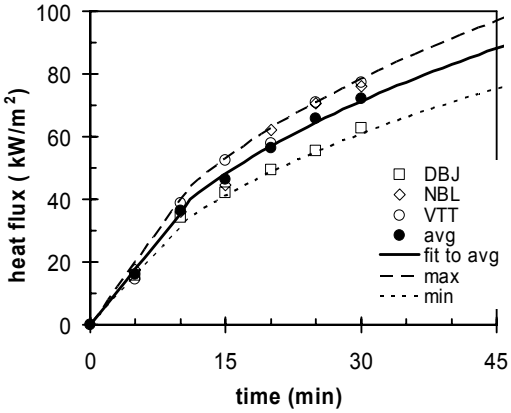

Figure 12. Heat flux values measured during standard temperature heating in three laboratories (Holm & Loikkanen 1981) (DBJ: Danish, NBL: Norwegian & VTT: Finnish).

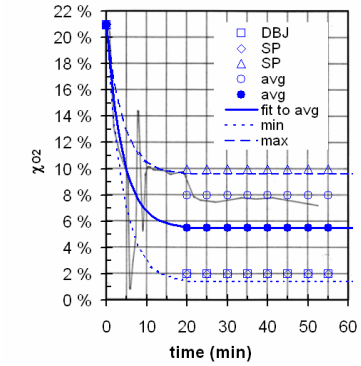

Figure 13. Oxygen concentration during standard temperature heating (Holm & Loikkanen 1981) (DBJ: Danish, NBL: Norwegian, SP: Swedish & VTT: Finnish laboratory).

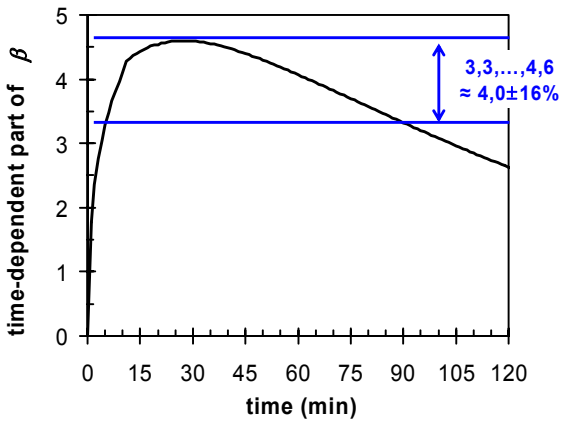

Figure 14. The average value of the time dependent part of the wood charring rate in standard temperature heat exposure.

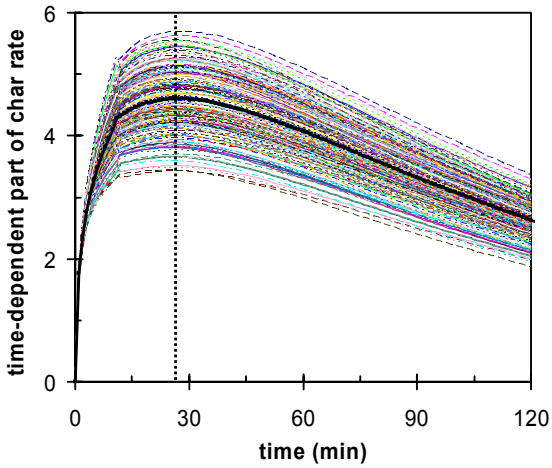

Figure 15. Stochastic model of the time dependent part of the wood charring rate in standard temperature heat exposure (a Monte Carlo sample of 200 samples).

The linearity of the charring in the standard temperature exposure becomes even more apparent when one considers the char depth as a function of time. To obtain the char depth we must integrate the time dependent part of the wood charring rate

$$I_{std}(t) = \int_0^t f(\chi_{O2}, t') \cdot \dot{q}''_{std}(t')^p \cdot \exp\left(-\frac{t'}{\tau}\right) dt' . \qquad (55)$$

This integral can be estimated numerically and the result including the variability is shown in Figure 16a. It can be seen that the evolution of this integral and thus the char depth can for any practical purposes be consider to be linearly in time with slope equal to 4,1 ± 25 %, or, by using curve fitting with the normal distribution (Figure 16b) we obtain

$$I_{std}(t) = \kappa_{std} \cdot t\,. \tag{56}$$

where

$$\kappa_{std} \propto N(3{,}8;0{,}45)\,. \tag{57}$$

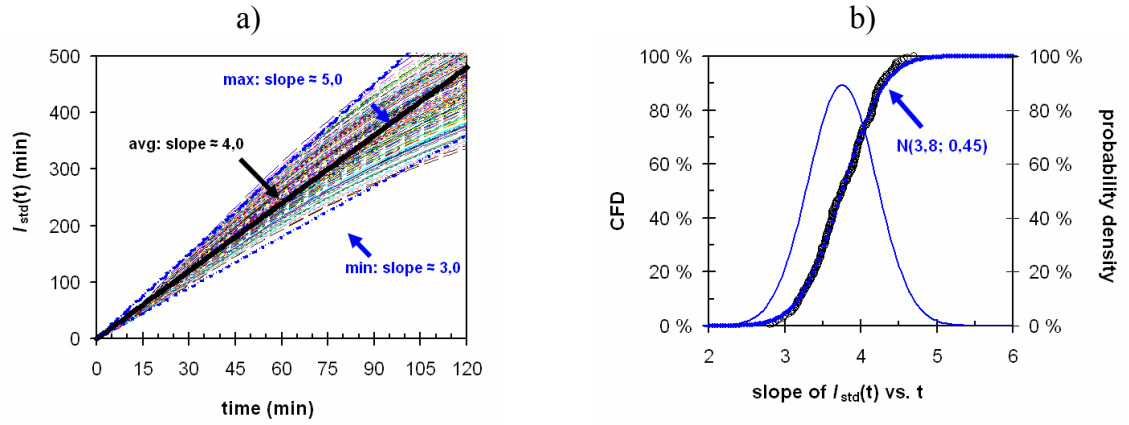

Figure 16. a) The average value of the time dependent part of the wood charring rate in standard temperature heat exposure. b) A detailed analysis of the slope by curve fitting using the normal distribution.

The equation for calculating the charring rate for the approximately linear char-depth time dependence encountered in the ISO heat exposure reads thus

$$\frac{\beta}{\text{mm/min}} = 60000 \cdot \frac{C}{(\rho + \rho_0)(A + B \cdot w)} \cdot \kappa_{std}\,, \tag{58}$$

where the random parameters A, B, C, ρ_0 and κ_{std} have the following distributions

$$C \propto \Delta(2{,}72;\, 5{,}45;\, 3{,}93)\ \text{kW/m}^2\,,$$

$$\rho_0 \propto N(465;93)\ \text{kgm}^{-3}\,,$$

$$\begin{cases} A \propto U(505;1095)\ \text{kJ/kg}\ (\text{average} = 800\ \text{kJ/kg}) \\ B \propto U(2430;2550)\ \text{kJ/kg}\ (\text{average} = 2490\ \text{kJ/kg}) \end{cases},$$

2.2.2.1 Experimental findings on the variability of wood charring rate under the standard fire exposure

In fire tests of wooden columns under loading carried out by Stanke (1969), the charring rate was observed to vary between 0,54 mm/min and 0,90 mm/min.

Son (1973) studied plywood specimen of different thicknesses, 12.7 mm, 15.9 mm and 2×12.7 mm, and obtained charring rates in the range 1,16–1,88 mm/min (data obtained from the review by Babrauskas (2004)).

Plywood of thickness of 19 mm has been studied Shoub and Son (1973) and Price (1977) who measured charring rates of 5,4 mm/min and 2,5 mm/min, respectively (data obtained from the review by Babrauskas (2004)).

Kallioniemi (1979) cites results of fire tests on glulam samples carried out in the former Soviet Union according to which the charring rate varies as follows:

- in 60 minute exposure minimum observed charring rate was 0,380 mm/min, maximum 0,968 mm/min and mean value was 0,567 mm/min,
- in 90 minute exposure minimum observed charring rate was 0,489 mm/min, maximum 0,945 mm/min and mean value was 0,689 mm/min.

In his own studies on loaded glulam specimens in the standard fire exposure, Kallioniemi (1979) observed charring rates of 0,47–0,73 mm/min.

For a 18,3-thick plywood, Fang (1982) observed a charring rate ranging between 1,04–1,14 mm/min (data obtained from the review by Babrauskas (2004)).

In the studies of White et al. (1984) on a 18,2 mm thick plywood a charring rate range 1,2–1,5 mm/min was observed (data obtained from the review by Babrauskas (2004)). White (2000) reported data on the charring rate of composite wooden products. For his data we can infer the following charring rate ranges: 0,63–0,75 mm/min for Douglas fir LVL and 0,53–0,65 mm/min for poplar LVL.

Richardson and Batista (2000) studied 38 mm thick timber decking with different gap sizes and observed charring rates varying from 1,13 mm/min to 8,4 mm/min (data obtained from the review by Babrauskas (2004)).

Oksanen (2005) has studied charring of loaded LVL (Kertopuu) specimens with different dimensions and observed that in the direction of the laminate, the charring rates vary between 0,50 mm/min and 0,69 mm/min and against the laminate direction measured charring rate was 0,48–1,05 mm/min. In another study with LVL specimens of different sizes (Oksanen 2005), charring rates between 0,55 mm/min and 1,4 mm/min were measured.

These data are summarised in Table 2 and Figure 17. It can be seen that the overall variability for the whole data set is characterised by a coefficient of variation (COV), *i.e.*, the standard deviation divided by the mean value, equal to *ca*. 60 %. For specific products, the scatter in the data may be smaller, *e.g.*, for glulam COV = 20 % and LVL COV = 27 %. For plywood, the data exhibit large scatter characterised by COV = 81 %. It is also seen that all the distributions are skewed.

Table 2. Experimental data on the charring rate of wood products in the standard fire exposure.

Specimen/test	β (mm/min)	average β (mm/min)	stdev. β (mm/min)	COV	Reference	Comment
Glulam	0.380	0.598	0.13	21 %	TsNIIEP 1971-1972	60 min. exposure, min. value; analysed as lognormal distribution
	0.968					60 min. exposure, max. value; analysed as lognormal distribution
	0.567					60 min. exposure, mean. value; analysed as lognormal distribution
Glulam	0.489	0.688	0.10	14 %		90 min. exposure, min. value; analysed as lognormal distribution
	0.945					90 min. exposure, max. value; analysed as lognormal distribution
	0.689					90 min. exposure, mean. value; analysed as lognormal distribution
						glulam: 0,64 (0,11) mm/min, COV = 18 %
Column	0.54	0.71	0.08	11 %	Stanke 1969	analysed as lognormal distribution
	0.90					analysed as lognormal distribution
	0.72					analysed as lognormal distribution
12.7 mm plywood	1.16	1.46	0.37	26 %	Son 1973	
15.9 mm plywood	1.34					
2×12.7 mm plywood	1.880					
19 mm plywood	5.4	3.95	2.05	52 %	Shoub & Son 1973	
	2.5				Price 1977	
Glulam beam, test A	0.733	0.66	0.08	13 %	Kallioniemi 1979	
Glulam column, test A	0.567					
Glulam beam, test A	0.667					
Glulam beam, test B	0.600	0.62	0.04	6 %		
Glulam beam, test B	0.600					
Glulam colunm, test B	0.667					
Glulam beam, test C	0.600	0.66	0.05	8 %		glulam: 0,60 (0,06) mm/min, COV = 9 %
Glulam beam, test C	0.667					
Glulam colunm, test C	0.700					
Glulam beam, test D	0.517	0.51	0.03	7 %		
Glulam beam, test D	0.500					
Glulam colunm, test D	0.550					
Glulam colunm, test D	0.467					
18.3 mm plywood	1.04	1.09	0.07	6 %	Fang 1982	
	1.14					18,3 & 18,2 mm plywood: 1,22 (0,20) mm/min, COV = 16 %
18.2 mm plywood	1.2	1.35	0.21	16 %	White et al. 1984	
	1.5					
Douglas fir LVL	0.63	0.69	0.08	12 %	White 2000	
	0.745					
Poplar LVL	0.53	0.59	0.08	14 %		
	0.65					
38 mm board, gap = 0 mm	1.13	3.03	2.70	89 %	Richardson 2000	
38 mm board, gap = 0 mm	1.560					
38 mm board, gap = 1 mm	2.900					
38 mm board, gap = 2 mm	8.400					
38 mm board, gap = 2.5 mm	2.100					
38 mm board, gap = 4 mm	2.100					without the 8,4 mm/min reading: 1,96 (0,67) mm/min, COV = 34 %
LVL Kertopuu beam 69x400	0.50	0.56	0.08	14 %	VTT LVL	at 15 minutes, ⊥ laminates
	0.500					
	0.580					
	0.660					
LVL Kertopuu beam 69x400	0.900	0.97	0.07	7 %	VTT LVL	at 10 minutes, // laminates
	0.910					
	1.000					
	1.050					⊥ laminates: 0,60 (0,05) mm/min, COV = 9 %
LVL Kertopuu beam 51x200	0.560	0.65	0.06	9 %	VTT LVL	at 15 minutes, ⊥ laminates
	0.660					
	0.670					
	0.690					// laminates: 0,76 (0,06) mm/min, COV = 8 %
LVL Kertopuu beam 51x200	0.490	0.56	0.07	12 %	VTT LVL	at 15 minutes, // laminates
	0.520					
	0.570					
	0.640					
joint of beam 90x270	0.747	0.65	0.14	22 %	VTT JointTests 90x270	side of the beam, at 15 minutes
	0.547					
joint of beam 90x270	1.400	1.09	0.44	40 %	VTT JointTests 90x270	bottom of the beam, at 15 minutes
	0.780					side: 0,75 (0,11) mm/min, COV = 14 %
joint of beam 115x315	0.900	0.86	0.06	7 %	VTT JointTests 115x315	side of the beam, at 15 minutes
	0.820					bottom: 1,06 (0,31) mm/min, COV = 30 %
joint of beam 115x315	1.067	1.03	0.06	6 %	VTT JointTests 115x315	bottom of the beam, at 15 minutes
	0.987					

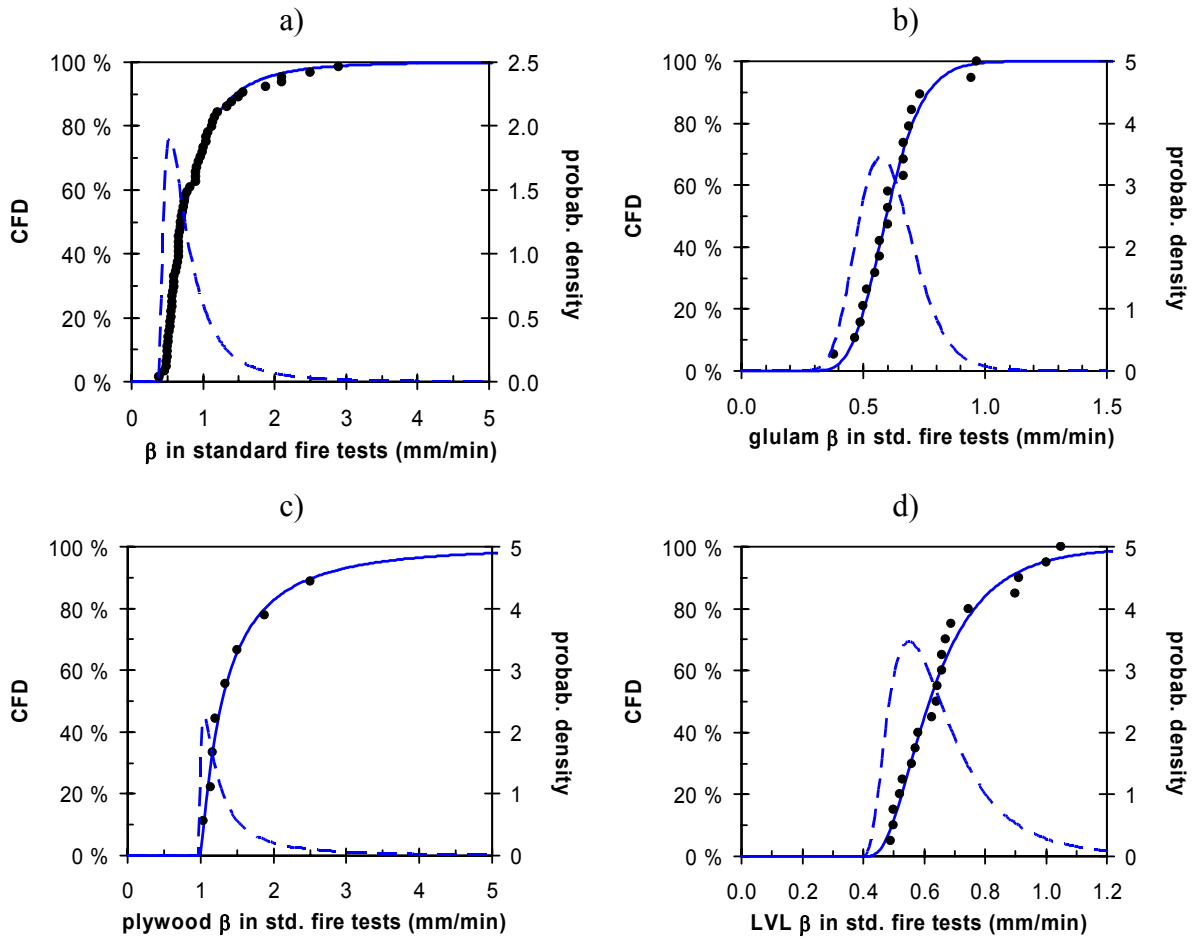

Figure 17. The data presented in Table 2 arranged as a cumulative frequency plot: a) the whole data set fitted with a shifted lognormal-distribution with mean = 0,89 mm/min, standard deviation = 0,55 mm/min and COV = 62 %, b) data for glulam fitted with a lognormal-distribution with mean = 0,57 mm/min, standard deviation = 0,12 mm/min and COV = 20 %, c) data for plywood fitted with a shifted lognormal-distribution with mean = 1,67 mm/min, standard deviation = 1,35 mm/min and COV = 81 % and d) data for LVL fitted with a shifted lognormal-distribution with mean = 0,66 mm/min, standard deviation = 0,18 mm/min and COV = 27 %.

2.2.2.2 Examples of the application of the calculation method in the case of the standard fire exposure

Now that we know the evolution of the time dependent part of the charring rate as well as the char depth we can evaluate charring rates for some wood products in the standard test, *e.g.*,

- low-density fibre board: density $\rho = 270$ kg/m^3, moisture $w = 10$ %;

- spruce timber: density $\rho = 440$ kg/m^3, moisture $w = 10$ %;
- pine timber: density $\rho = 560$ kg/m^3, moisture $w = 10$ %;
- medium-density fibre board: density $\rho = 700$ kg/m^3, moisture $w = 10$ %.

The results are shown as distributions in Figure 18. Table 3 summarises the characteristics of the distributions. The two different distributions employed , the three-parameter gamma distribution with the probability density *f(x)* and the cumulative frequency distribution $F(x)$ (CFD) given by

$$\begin{aligned} f_\lambda(x;a,b,x_{\min}) &= \frac{1}{\Gamma(a)\cdot b^\alpha}(x-x_{\min})^{a-1}\exp\left(-\frac{x-x_{\min}}{b}\right), \text{ when } x \geq x_{\min}, \text{ 0 otherwise,} \\ F_\lambda(x;a,b,x_{\min}) &= \int_0^x f(x';a,b,x_{\min})dx' \end{aligned} \quad (59)$$

and the logarithmically normal distribution with the probability density *f(x)* and the cumulative frequency distribution $F(x)$ (CFD) given by

$$\begin{aligned} f_{LN}(x;a,b) &= \frac{1}{x\cdot b\cdot\sqrt{2\pi}}\exp\left(-\left(\frac{\ln x - a}{\sqrt{2}\cdot b}\right)^2\right), \text{ when } x \geq 0, \text{ 0 otherwise,} \\ F_{LN}(x;a,b) &= \int_0^x f(x';a,b)dx' \end{aligned} \quad (60)$$

give virtually the same results. It is seen that the coefficient of variation, *i.e.*, the standard deviation divided by the mean value, is the same, 27 %, for all four examples considered. This is general agreement with the experimental values shown in Table 2 and Figure 17.

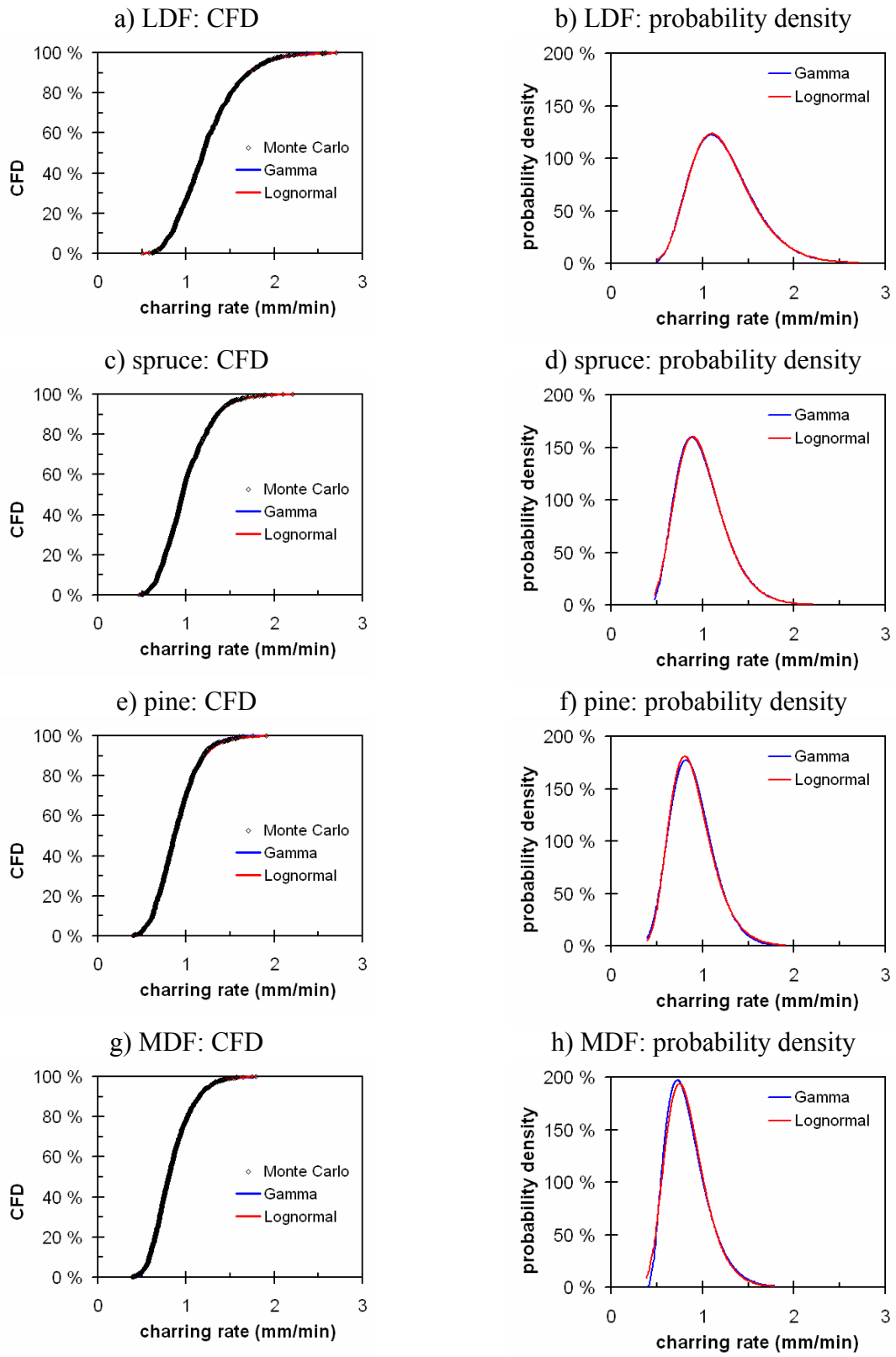

Figure 18. Examples of variability of the charring rate in the standard fire exposure of LDF-board (a & b), spruce timber (c & d), pine timber (e & f) and MDF-board (g & h).

Table 3. Characteristics of the distribution used to describe the variability of the wood charring rate in the standard fire exposure.

Species	**Three-parameter gamma distribution**	**Log-normal distribution**
Low-density fibre board density ρ = 270 kg/m^3, moisture w = 10 %	a = 6,51 b = 0,137 mm/min x_{min} = 0,344 mm/min mean[a)] = 1,23 mm/min median[b)] = 1,10 mm/min std.deviation[c)] = 0,34 mm/min COV[d)] = 28 %	a = 0,174 b = 0,283 mean[e)] = 1,24 mm/min median[f)] = 1,19 mm/min std.deviation[g)] = 0,36 mm/min COV = 29 %
Spruce timber density ρ = 440 kg/m^3, moisture w = 10 %	a = 5,64 b = 0,116 mm/min x_{min} = 0,355 mm/min mean = 1,00 mm/min median = 0,88 mm/min std.deviation = 0,27 mm/min COV = 27 %	a = -0,041 b = 0,269 mean = 1,00 mm/min median = 0,96 mm/min std.deviation = 0,27 mm/min COV = 27 %
Pine timber density ρ = 560 kg/m^3, moisture w = 10 %	a = 12,45 b = 0,0661 mm/min x_{min} = 0,067 mm/min mean = 0,89 mm/min median = 0,82 mm/min std.deviation = 0,23 mm/min COV = 26 %	a = -0,145 b = 0,264 mean = 0,90 mm/min median = 0,86 mm/min std.deviation = 0,24 mm/min COV = 27 %
Medium-density fibre board density ρ = 700 kg/m^3, moisture w = 10 %	a = 4,06 b = 0,113 mm/min x_{min} = 0,381 mm/min mean = 0,84 mm/min median = 0,73 mm/min std.deviation = 0,23 mm/min COV = 27 %	a = -0,218 b = 0,265 mean = 0,83 mm/min median = 0,80 mm/min std.deviation = 0,23 mm/min COV = 27 %

a) Mean of the three-parameter gamma distribution = $a \cdot b + x_{min}$.

b) Median of the three-parameter gamma distribution = $x_{min} + F_{\gamma}^{-1}(0{,}5, a, b)$.

c) Standard deviation of the three-parameter gamma distribution = $b\sqrt{a}$.

d) COV = (standard deviation)/mean.

e) Mean of the log-normal distribution = $\exp\left(a + \frac{1}{2}b^2\right)$.

f) Median of the log-normal distribution = $F_{LN}^{-1}(0{,}5, a, b)$.

g) Standard deviation of the log-normal distribution = $\exp\left(a + \frac{1}{2}b^2\right)\sqrt{\exp\left(b^2\right) - 1}$.

3. Application to assessment of failure probability of a load-bearing glulam beam

The description of the wood charring rate derived in the previous Chapter finds use in probabilistic approaches to assessment of fire safety (Hietaniemi *et al*. 2004, Hostikka & Keski-Rahkonen 2003). As compared to the deterministic approaches to assessment of fire safety, the probabilistic approaches have the virtue that they can take into account the inherent stochastic nature of the fire phenomenon and the related hazards. As there is a great deal of variability and uncertainties involved in the fire and the related phenomena and our understanding of these subjects it is well justified to argue that it is as important to be able to quantity the uncertainties as it is to quantify the phenomena themselves. The price one has to pay for the enhanced predictive power of the probabilistic approaches to assessment of fire safety is that the analysis procedures become more complex, which becomes manifest, *e.g*., when we compare the formulae of the previous Chapter to the single-value charring rate expression of the deterministic approaches. This, however, does not imply that the probabilistic approaches would be too cumbersome for practical fire-safety engineering work. All it takes is that the problem has been tackled once and coded into a software where after any similar problem can be solved in a routine manner. When it comes creating the software, there packages such as the Probabilistic Fire Simulator (PFS) developed by the Fire Research Group of VTT (Hietaniemi *et al*. 2004, Hostikka & Keski-Rahkonen 2003, Hostikka *et al*. 2003) readily available that can be used as a platform when developing software to solve specific problems.

3.1 Overview of the procedure

The procedure of the assessment of the failure probability goes as follows:

- Calculate using fire simulation the heat release rate (HRR) and the temperature (T_g) which exposes the structures as well as the flow velocity (v) and the smoke density (k) around the structures.

- Calculate the heat exposure, *i.e*. the heat flux $\dot{q}_2''$, to structures on the basis of the quantities T_g, v and k:

$$\dot{q}_e'' = h \cdot \left(T_g - T_\infty\right) + \phi\sigma\varepsilon_r\left(T_g^4 - T_\infty^4\right), \tag{61}$$

where T_∞ is the ambient temperature[4], ϕ is the view factor between the flames and/or hot gases and the structure and ε_r is the resultant emissitivity for the flames and/or hot gases and the structure. For a structural member immersed in the smoky hot gas layer, $\phi = 1$, and $\varepsilon_r = \varepsilon_s$ = the emissivity of the member are suitable choices.

- Calculate the charring rate β by Monte Carlo simulation using expression (32).
- Calculate the char depth d by integrating the β over the relevant time period and subtract d from the initial dimensions b_{init} (width) and h_{init} (height) to obtain the reduced section properties as a function of time.
- Construct the limit state function g, *i.e.*, member mechanical resistance minus the load, for the loading conditions considered.
- Member failure takes place at the time when g becomes negative.
- The estimate for failure time distribution is obtained from the Monte Carlo sample.

3.2 Application example

The building considered in this study is a shop located in South-West part of Finland. It consists basically of a single space with length of 50 m, width 34 m and height 5,5 m. The building has a timber beam-column structure of glued laminated wood. Glulam columns support 17 m long beams which compose the roof structure. The dimensions of the beam are b_{init} = 165 mm and h_{init} = 1215 mm.

Deterministic design calculations using 50 % of the snow load characteristic to that part of Finland, i.e., 1,4 kN/m^2, show that unprotected the beam would survive standard fire exposure for 30 minutes.

[4] Note that the derivation of the expression (32) for charring rate is based on the gross heat flux impinging on the specimen and thus, one must use here the heat flux that corresponds to a surface at its initial temperature T_∞.

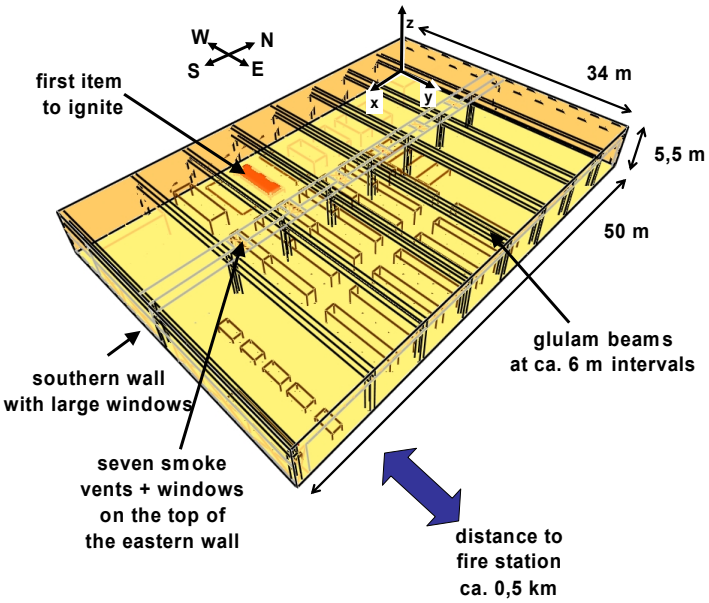

Figure 19. The target building. The principal fire safety measures are the smoke vents, which activate at 100 °C and simultaneously give an alarm signal to the fire station located in the near vicinity of the building.

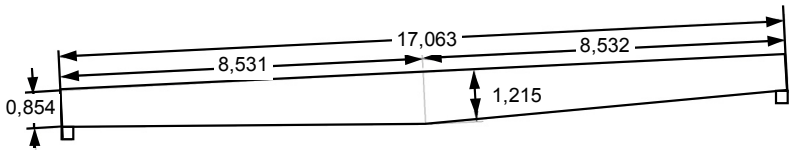

Figure 20. The glulam beam spanning between the columns.

We have analysed several fire scenarios in this building using both a deterministic fire simulation with the FDS 3 (McGrattan *et al*. 2002a, McGrattan *et al*. 2002b) and FDS 4 (McGrattan 2004a, McGrattan 2004b) program and a probabilistic fire simulation using the PFD program. Some of these scenarios have been dealt with in earlier presentations (Hietaniemi & Korhonen 2004a, Hietaniemi & Korhonen 2004b). In this example we consider only one fire scenario, a fire which grows hot enough to break the large windows on the south wall of the building. In this case the HRR may grow up to hundreds of megawatts (Figure 21). It should be noted that the fire development is principally governed by the potential breakage of the large windows and the particular scenario we are considering here is one in which the temperature required for the window breakage *and fallout* is 300 °C. This is actually a rather low temperature for major glass breakage leading to a fallout which will be taken into account when we estimate probability of this particular fire scenario needed in the assessment of the overall probability of structural failure.

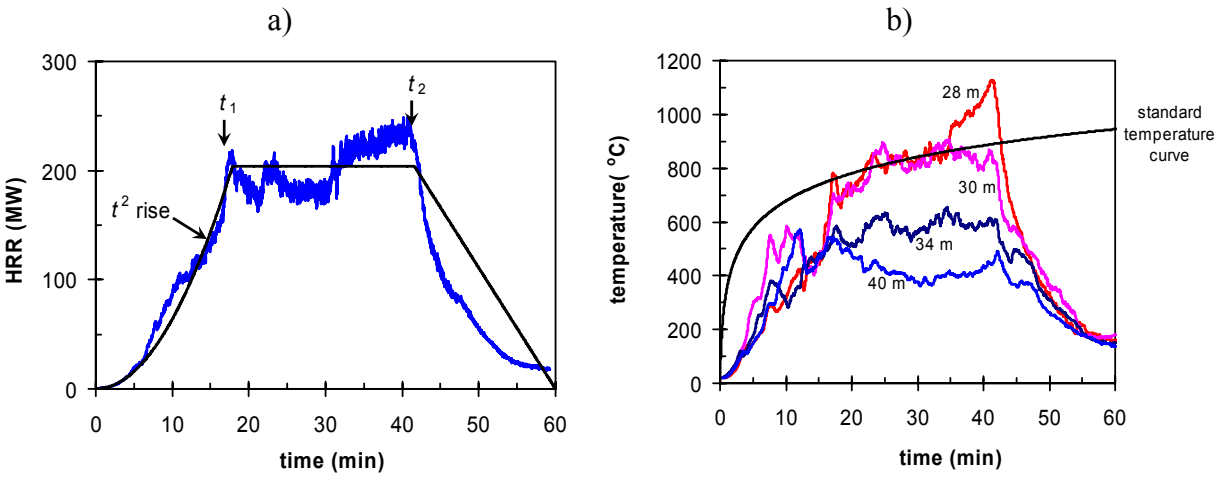

Figure 21. Example of the results of the deterministic FDS4 fire simulations of the scenario in which the large windows on the south wall break at 300 °C: a) the heat release rate and b) hot gas temperatures at different position along the x-direction at the centre of the building at height z = 4,5 m.

We convert the HRR results of the deterministic fire simulation to stochastic HRR curves as follows

- first we analyse the HRR obtained from the FDS 4 simulations by an analytical model with an initial time dependence of the t^2-form with growth time t_g followed by a steady-HRR-phase at maximum HRR between times t_1 and t_2 and a linear decay phase after the time t_2 (see Figure 22a);
- the next step is to treat the parameters of the analytical expression as random quantities with their scatter characterised by the selected statistical distributions listed in Table 4;
- the final step is to carry out the probabilistic fire simulations to obtain a Monte Carlo sample of the HRR and gas temperature curves (Figure 22).

Table 4. Description of the distributions used to characterise the stochastic nature of the design fire.

Quantity	**Distribution**
Growth time t_g	Lognormal distribution with median = 300 s and std.deviation = 100 s
Maximum HRR	Evaluated on the basis of probabilistic fire simulations with the heat release rate per surface area, growth time, window breaking time and the portion of fallen out window as random parameters. The resulting distribution can be fitted using the 3-parameter Weibull distribution[5] with minimum = 30 MW, median = 227 MW and std.deviation = 87 MW.
Time t_1	Moment when the initial growing HRR reaches the max HRR: a dependent variable calculated from t_g and max. HRR.
Time t_2	Time when the cumulated heat release (MJ) equals the total amount of available combustible energy Q_{tot} minus the heat release during the decay phase Q_{dec}, which is based on the predetermined portion p of Q_{dec} of Q_{tot}. Following the Eurocode 1 (CEN 2002b), we assume that the mean value on p is 70 %; the variability of p is characterised by the uniform distribution ranging from 60 % to 80 %.

[5] The probability density of the Weibull distribution is $f(x) = \left(\frac{\alpha}{\beta^{\alpha}}\right) \cdot \left(x - x_{\min}\right)^{\alpha-1} \cdot \exp\left(-\left(\frac{x - x_{\min}}{\beta}\right)^{\alpha}\right)$ and the cumulative distribution function $F(x) = 1 - \exp\left(-\left(\frac{x - x_{\min}}{\beta}\right)^{\alpha}\right)$. The median equals $x_{\min} + \beta(\ln 2)^{1/\alpha}$ and the standard deviation $\beta\sqrt{\Gamma\left(\frac{2}{\alpha}+1\right) - \left[\Gamma\left(\frac{1}{\alpha}+1\right)\right]^2}$ where Γ(x) is the gamma function.

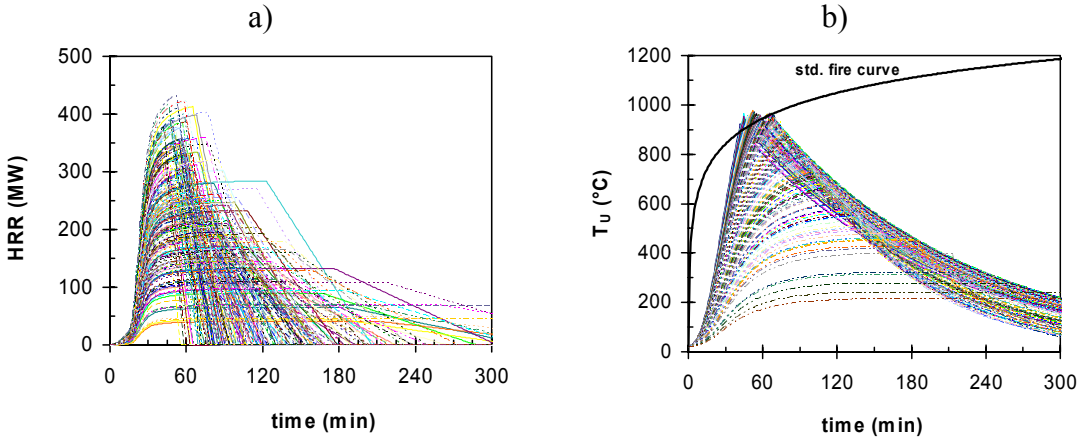

Figure 22. Examples of the PFS probabilistic fire simulations of the scenario in which the large windows on the south wall break at 300 °C: a) the heat release rate and b) hot gas temperatures at the centre of the building at height z = 4,5 m (in both cases, 200 curves of the Monte Carlo sample of size 1000 are shown).

The FDS fire simulations show that the hot gas layer is quite smoky with a typical value of the extinction coefficient being 2–4 m^{-1} and hence, the regarding radiative heat transfer, the gases may be considered as "black", *i.e.*, having emissivity close to 1: in the Monte Carlo simulations we use the uniform distribution ranging from 0,9 to 1,0 for the emissivity. The most rigorous treatment of the convective heat transfer would be to analyse it on the basis of the fluid flow speed around the structures. Here, however, we assume that the heat transfer coefficient is about 25 $Wm^{-2}K^{-1}$ (uncertainties in the heat transfer coefficient are characterised by drawing its values from a triangular distribution with minimum value of 20 $Wm^{-2}K^{-1}$, maximum value of 35 $Wm^{-2}K^{-1}$ and peak value of 25 $Wm^{-2}K^{-1}$). The resulting heat fluxes are shown in Figure 23a.

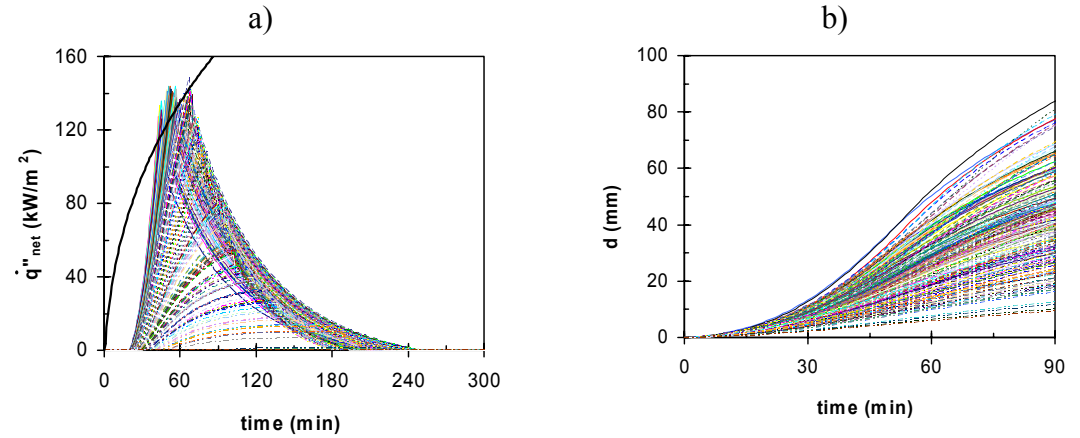

Figure 23. a) The heat fluxes and b) corresponding char depths (in both cases, 200 curves of the Monte Carlo sample of size 1000 are shown).

The char depths corresponding to the heat fluxes are obtained by integrating the charring rate expression (39), see Figure 23b. Figure 24 shows an analysis of how the char depth evolves during the fire exposure: at 30 minutes the mean value is 6,8 mm and standard deviation 2,2 mm, at 60 minutes the mean value is 25 mm and standard deviation 9,7 mm and at 60 minutes the mean value is 42 mm and standard deviation 16 mm.

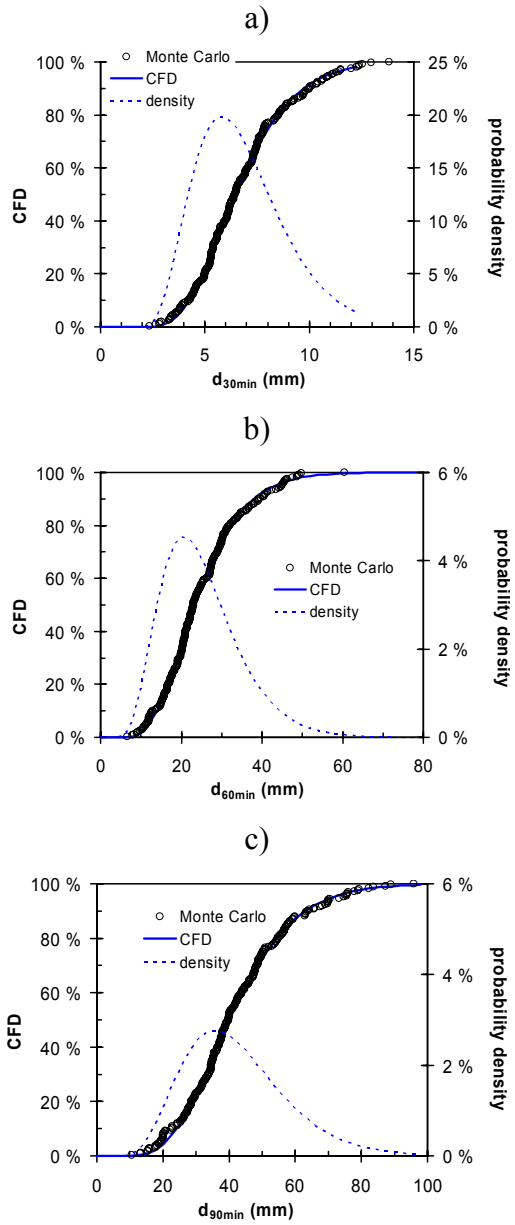

Figure 24. Analyses of the char depths: a) at 30 minutes, b) at 60 minutes and c) at 90 minutes.

The load-bearing capacity of the beam is calculated on the basis of the following limit-state function (Toratti & Turk 2005, Hietaniemi & Korhonen 2004a, Hietaniemi & Korhonen 2004b)

$$g = F \times k_{\mathrm{mod},fi} \times k_{m,\alpha} - \left(\frac{N_{xp} \times (G+Q)}{b_{red} \times h_{red}} + \frac{6 \times M_{yp} \times (G+Q)}{b_{red} \times h^2{}_{red}}\right) \times \mathrm{model} \quad , \tag{62}$$

where the quantities treated as random variables are

- G = permanent load (normal distribution with mean 3,65 kN/m and coefficient of variation V_G = 0.05);
- Q = snow load (the local measured snow load distribution for the particular town in the South-Western part of Finland, see Figure 25)
- F = glulam strength (bending and shear) (log-normal distribution with mean 50,4 N/mm^2 and coefficient of variation V_F = 0.15);
- model = model uncertainty (distribution with mean 1.0 and coefficient of variation V_m = 0.05);
- b_{red} and h_{red} : the reduced section dimensions for width and height, respectively, calculated using the calculated char depths (see Figure 23b). Their initial values were allow to vary by 1 % (normal distribution).

and the quantities treated as constant variables are:

- $k_{mod,fi}$ = 1,0; $k_{m,\alpha}$ = 0.79 (constant);
- N_{xp} = 0.346 [kN per unit load (kN/m)];
- M_{yp} = 29.144 [kNm per unit load (kN/m)];
- α = 2.5^o (constant).

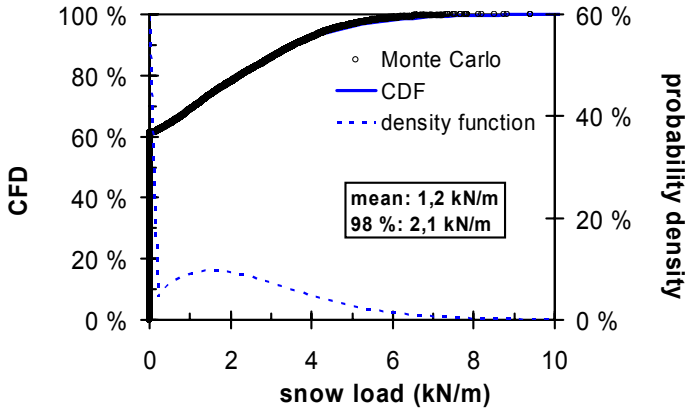

Figure 25. Statistical distribution of the snow load for the location of the building. This distribution applies for the whole year and hence the chance of zero snow load is a bit more than 60 %. The distribution is based on the measurements of the water value of snow in South-West Finland (Perälä & Reuna 1990).

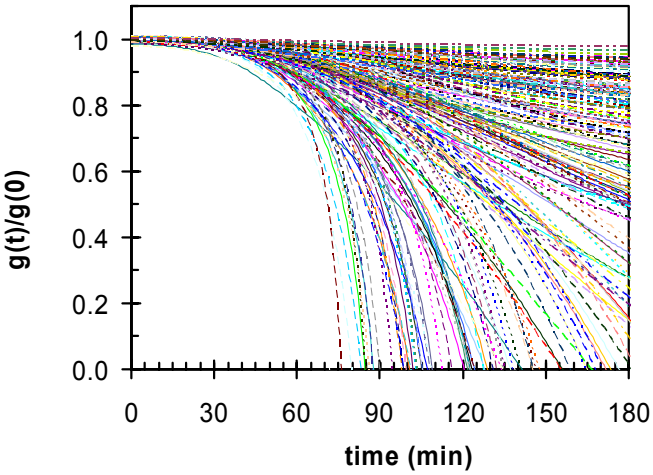

Figure 26. Limit state functions (a sample of 200 curves from the total of 1000 Monte Carlo samples).

The dependence of the limit-state functions on time is exemplified in Figure 26. Failure time of the beam is the time when limit-state function g becomes negative. The distribution of the failure times deduced from the zero-crossings of the limit-state function is shown in Figure 27. The failure probabilities that may be read from this curve are *probabilities of failure per one design fire in the case where no actions are taken to fight the fire*. It is seen that this nominally R30 beam tolerates the natural fire exposure quite well: at 60 minutes, the failure probability equals zero and at 90 minutes

it is about 3 % and at 120 minutes ca. 13 %. The beam fails in only about 37 % of the design fires (the failure probability saturates at 37 % at long times).

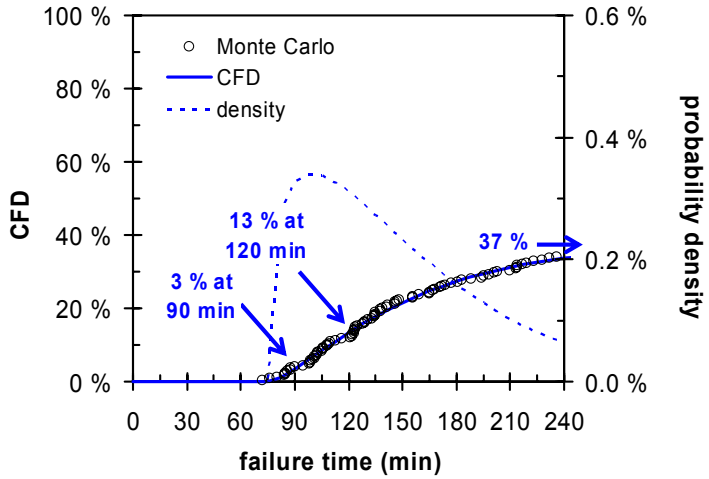

Figure 27. Distribution of the beam failure time. The probabilities depicted by the CFD curve are probabilities of failure per one design fire in the case where no actions are taken to fight the fire.

To obtain the absolute probability of failure of the beam, e.g., per one fire or per one year, we must

1) Scale the probabilities shown in Figure 27 down by the probability of the design fire which comprises two factors

   a) the probability of a fire of any severity in the building and

   b) the probability of a fire of such severity as the design fire we have used in our calculations.

2) Assess the probability that the fire brigade will extinguish the fire before it chars so severely that it fails.

The probability of a fire in a shop may be deduced from fire statistics. In Finland, Tillander and Keski-Rahkonen have carried out comprehensive analysis of the fire statistics collected into the PRONTO database of the Ministry of the Interior: their results include the fire ignition frequency densities for different building categories (Tillander & Keski-Rahkonen 2001, Tillander 2004) as well as the fire brigade response times (Tillander & Keski-Rahkonen 2000). According to their results, the fire ignition

frequency density[6] for a 1700-m^2 grocery is $5 \cdot 10^{-6}$ fires/m^2/year. Thus, the annual fire ignition frequency is $1700 \times 5 \cdot 10^{-6}$ fires/year = $8{,}5 \cdot 10^{-3}$ fires/year. Our design fire is a very severe, most likely to take place due to an action of an arsonist inside the building, and thus we assign a probability of 1 % to the design fire, *i.e.*, we assume that only one fire out of 100 fires reported to fire brigades has the potential of growing as severe as our design fire. Thus, the frequency of our design fire is roughly $1 \cdot 10^{-4}$ per year or once in ten thousand years. Note that here we do not yet include the influence of the attempts to suppress the fire by the fire brigade.

The actions of the fire brigade can be taken into account by the Time-Dependent Event Tree (TDET) method developed at VTT (Korhonen *et al*. 2002, Hietaniemi *et al.* 2004). It enables also to assess the influence of active or passive fire safety measures to the probability of harm caused by the fire. We have analysed the following cases:

- With respect to the active fire safety measures we have analysed the following three different types of alarming systems:
  - the existing system in which there is an automatic alarm to the fire brigade when the smoke vents activate at 100 °C, operational reliability 95 %,
  - detection and alarming triggered at 100 °C, operational reliability 99 %,
  - detection and alarming triggered at 57 °C, operational reliability 95 %.
- With respect to passive fire safety provisions, the cases we consider are the beam as it is in the building and a bulkier and hence more fire endurable beam with a cross-section of 190×1260 mm^2. The failure probability of such beam is shown in Figure 28.

[6] As the Finnish fire statistics are collected from fire brigades, these fires are in which the fire brigade has been alarmed.

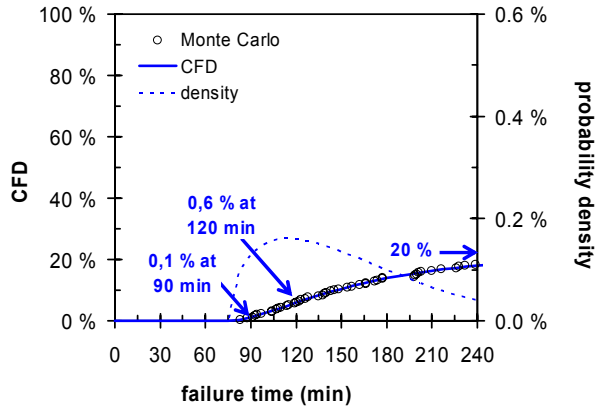

Figure 28. Distribution of the beam failure time for a beam with a larger cross section, 190×1260 mm^2.

In each case we consider the occupied hours and the unoccupied hours separately as there is a distinct difference in the detection of the fire: while during the occupied hours, the fire may be detected either by detectors or humans, during the unoccupied times the fire detection will most probably take place via detectors. In calculating the total probability, we weight the probabilities for occupied hours by a factor (5×14 + 7)/7×24 = 0,46 (from Monday to Friday the store is open from 7 am. to 9 pm. and on Saturday from 7 am. to 2 pm.) and probabilities for the unoccupied hours by a factor of 0,54.

The results of the TDET analysis are given in Table 5 and Figure 29. The vertical line in Figure 29 depicts the failure probability limit of $70 \cdot 10^{-6}$ per building lifetime as stipulated in the Eurocode 0 (CEN 2002a). It may seen that the beam survives the whole fire duration with a sufficiently low probability of failure in all cases. Regarding the fire safety measures, improving the reliability of the fire detectors is the most efficient measure. Improving the fire resistance of the beam by selecting a larger cross section ranks second best of the fire safety measures that we consider in this study. Improving the sensitivity (lowering the activation temperature) does not seem to be an efficient way to improve safety in this particular case building.

Table 5. Summary of the TDET analysis results for the different cases considered. The design fire frequency is $1 \cdot 10^{-4}$ year^{-1}.

Case		occupied hours	unoccupied hours	combined value: failure probability per design fire	absolute annual failure frequency (1/year)	absolute life-time failure frequency (1/50 years)
100 °C, 95 %, normal beam	**90 min**	0,0003 %	0,20 %	0,11 %	$0{,}11 \cdot 10^{-6}$	$6 \cdot 10^{-6}$
	120 min	0,0022 %	0,72 %	0,39 %	$0{,}39 \cdot 10^{-6}$	$20 \cdot 10^{-6}$
	whole fire duration	0,0029 %	1,5 %	0,81 %	$0{,}81 \cdot 10^{-6}$	$41 \cdot 10^{-6}$
100 °C, 99 %, normal beam	**90 min**	0,0001 %	0,050 %	0,027 %	$0{,}027 \cdot 10^{-6}$	$1 \cdot 10^{-6}$
	120 min	0,0006 %	0,19 %	0,10 %	$0{,}10 \cdot 10^{-6}$	$5 \cdot 10^{-6}$
	whole fire duration	0,0012 %	0,38 %	0,21 %	$0{,}21 \cdot 10^{-6}$	$11 \cdot 10^{-6}$
57 °C, 95 %, normal beam	**90 min**	0,0001 %	0,18 %	0,097 %	$0{,}10 \cdot 10^{-6}$	$5 \cdot 10^{-6}$
	120 min	0,0005 %	0,67 %	0,36 %	$0{,}36 \cdot 10^{-6}$	$18 \cdot 10^{-6}$
	whole fire duration	0,0010 %	1,4 %	0,76 %	$0{,}76 \cdot 10^{-6}$	$38 \cdot 10^{-6}$
100 °C, 95 %, larger cross-section beam	**90 min**	0,0001 %	0,069 %	0,037 %	$0{,}037 \cdot 10^{-6}$	$2 \cdot 10^{-6}$
	120 min	0,0003 %	0,33 %	0,18 %	$0{,}18 \cdot 10^{-6}$	$9 \cdot 10^{-6}$
	whole fire duration	0,0006 %	0,75 %	0,41 %	$0{,}41 \cdot 10^{-6}$	$21 \cdot 10^{-6}$

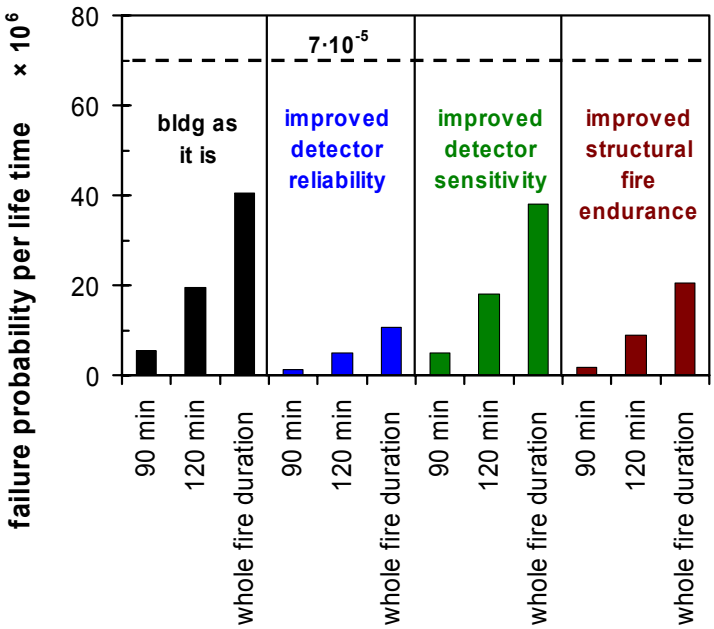

Figure 29. Beam failure probabilities during the life time of 50 years of the building for the different fire-safety-provision cases.

4. Summary

This report presents a probabilistic model for wood charring rate and an application of the model to assess fire resistance of a wooden load-bearing beam. The model is an empical one, based on quantification of the dependence of the wood charring rate on the principal physical factors governing the charring process. These factors include the influence of the heat flux exposing the wood surface, the wood density and moisture content as well as the ambient oxygen concentration. The application introduces a novel approach to assess the endurance of a wooden structural member in a natural fire conditions, which uses probabilistic fire simulation to quantify the heat exposure and the char depth of the structural member. The principal result of the approach is the time evolution of the conditional failure probability of failure of the structural wooden member, which can be further elaborated by incorporating into the analysis the statistical and modelling results determining the frequency of the conditioning factor, i.e., the occurrence of a fire with sufficient severity to potentially compromise the structural safety.

Acknowledgements

The authors gratefully acknowledge the financing to the work by the National Technology Agency of Finland (Tekes) and VTT Building and Transport.

References

Babrauskas, V. 2004. Wood Char Depth: Interpretation in Fire Investigations. International Symposium on Fire Investigation, Fire Service College, Moreton-in-Marsh, United Kingdom, 28th June 2004. (http://www.doctorfire.com/ WoodCharring.pdf, referred to 13th April 2005)

Bevington, P. R. & Robinson, D. K. 1992. Data Reduction and Error Analysis for the Physical Sciences. Boston USA: WCB/McGraw-Hill. 328 p.

CEN 2002a. EN 1990. Eurocode – Basis of structural design. Brussels: CEN. 57 p. (EN 1990: 2002.).

CEN 2002b. Eurocode 1: Actions on Structures – Part 1–2: General Actions – Actions on structures exposed to fire. Brussels: CEN. 59 p. (EN 1991-1-2: 2002 E.).

de Souza Costa, F. & Sandberg, D. 2004. Mathematical Model of a Smoldering Log. Combustion and Flame, Vol. 139, 227–238.

Dunlap, F. The Specific Heat of Wood. 1912. Washington DC. US Department of Agriculture, Bulletin No. 110, 1912.

Fang, J. B. 1982. Fire Endurance Test of Selected Residential Floor Constructions. National Bureau of Standards, Gaithersburg MD, USA. (NBSIR 82 2488).

Fredlund, B. 1988. A Model for Heat Transfer and Mass Transfer in Timber Structures During Fire. A Theoretical, numerical and experimental study. Lund: Lund University. (Report LUTVDG/(TVBB-1003)). 254 p.

Hietaniemi, J., Korhonen, T., Joyeux, D. & Ayme, N. 2004. Risk-based Fire Safety Engineering Approach to Obtain Balanced Structural Fire Resistance Requirements. In: Bradley, D., Drysdale, D. & Molkov, V. Fire and Explosion Hazards, Proceedings of the Fourth International Seminar. Londonderry, Northern Ireland, UK, September 8–12, 2003. Belfast, Northern Ireland, UK: University of Ulster. Pp. 505–514. ISBN 85923 186 1.

Hietaniemi, J. & Korhonen, T. 2004a. A case study of performance of load-bearing wooden structures in natural fire. Proceedings of the 8th World Conference on Timber Engineering, WCTE 2004, Volume II, Lahti, June 14–17, 2004. Helsinki: RIL, VTT, Wood Focus. Pp. 329–334.

Hietaniemi, J. & Korhonen, T. 2004b. Study of performance of load-bearing wooden structures in natural fire. Wood and Fire Safety, 5th International Scientific Conference, 18–22 April 2004, Strbské Pleso. Technical University in Zvolen, Department of Fire Protection, Faculty of Wood Sciences and Technology. 2004. 9 p.

Hietaniemi, J., Hostikka, S. & Korhonen, T. 2004. Probabilistic Fire Simulation. In: Almand, K. H. (Ed.). Proceedings of the 5th International Conference on Performance-Based Codes and Fire Safety Design Methods. October 6–8, 2004. Luxembourg. Bethesda, MD. USA. Society of Fire Protection Engineers. Pp. 280–291.

Holm, C. & Loikkanen, P. 1981. Joint Investigation of Vertical Furnaces in Nordic Countries. VTT Research Notes 56/1981. 52 p. + app. 6 p.

Hostikka, S. & Keski-Rahkonen, O. 2003. Probabilistic simulation of fire scenarios. Nuclear Engineering and Design, Vol. 224. Pp. 301–311.

Hostikka, S., Keski-Rahkonen, O. & Korhonen, T. 2003. Probabilistic Fire Simulator. Theory and User's Manual for Version 1.2. Espoo, VTT Building and Transport. VTT Publications 503. 72 p. + app. 1 p. ISBN 951-38-6235-6; 951-38-6236-4. http://www.vtt.fi/inf/pdf/publications/2003/P503.pdf

Kallioniemi, P. Kantavien puurakenteiden palonkestävyydestä (On the fire resistance of load-bearing wooden constructions). Licentiate of Technology Thesis, Helsinki University of Technology, 1979. (In Finnish)

Koch, P. 1969. Specific Heat of Oven-dry Spruce Pine Wood and Bark. Wood Science, Vol. 1, No. 4. Pp. 203–214.

Korhonen, T., Hietaniemi, J., Baroudi, D. & Kokkala, M. 2002. Time-Dependent Event-Tree Method for Fire Risk Analysis: Tentative Results. 7th International Symposium of Fire Safety Science. Boston: 16–21 June 2002. Pp. 321–332.

McGrattan, K. B. (Ed.). 2004a. Fire Dynamics Simulator (Version 4): User's Guide. 104 p. (NIST Special Publication 1019).

McGrattan, K. B. (Ed.). 2004b. Fire Dynamics Simulator (Version 4): Technical Reference Guide. 101 p. (NIST Special Publication 1018).

McGrattan, K. B., Baum, H. R., Rehm, R. G., Hamins, A., Forney, G. P., Floyd, J. E., Hostikka, S. & Prasad, K. 2002a. Fire Dynamics Simulator (Version 3) – Technical

Reference Guide. Gaithersburg, MD. USA: National Institute of Standards and Technology. 51 p. (NISTIR 6783, 2002 Ed.).

McGrattan, K. B., Forney, G. P., Floyd, J. E., Hostikka, S. & Prasad, K. 2002b. Fire Dynamics Simulator (Version 3) – User's Guide. Gaithersburg, MD. USA: National Institute of Standards and Technology. 81 p. (NISTIR 6784, 2002 Ed.).

Mikkola, E. 1988. Unpublished time-series data on charring of several wood product under constant heating in the cone calorimeter.

Mikkola, E. 1989. Puupinnan syttyminen (Ignition of wooden surface). Espoo: VTT Tiedotteita 1057. 48 p. ISBN 951-38-3589-8. (In Finnish)

Mikkola, E. 1990. Charring of wood. Espoo: VTT Tutkimuksia 689. ISBN 951-38-3711-4. 40 p.

Njankouo, J. M., Dotreppe, J.-C. & Franssen, J.-M. 2004. Experimental study of the charring rate of tropical hardwoods. Fire and Materials, Vol. 28. Pp. 15–24.

Nurbakhsh, S. 1989. Thermal decomposition of charring materials. PhD dissertation. East Lansing: Michigan State University. 256 p.

Ohnemiller, T. J., Kashiwagi, T. & Werner, K. 1987. Wood gasification at fire level heat fluxes. Combustion and Flame, Vol. 69. Pp.155–170.

Oksanen, T. 2005. Privite communication.

Parker, W. J. 1985. Development of a Model for the Heat Release Rate of Wood. Gaithersburg, MD: National Bureau of Standards. 108 p. (NBSIR 85-3163).

Perälä, J. & Reuna, R. 1990. Lumen vesiarvon alueellinen ja ajallinen vaihtelu Suomessa (Regional and temporal variation of snow water value in Finland). Vesi ja ympäristöhallitus. Julkaisuja – sarja A 56. Helsinki 1990. (In Finnish)

Price, W. R. 1977. ASTM E 119-76 Fire Endurance Test. Floor-Ceiling Assembly. Wood Trusses with Plywood Floor. Design FC-240. Factory Mutual Research, Norwood, MA, USA. Job identification J.I. OA8Q8.AC(4610).

Quintiere, J.G. & Harkleroad, M.T. 1985. New Concepts for Measuring Flame Spread Properties, Fire Safety: Science and Engineering, ASTM STP882, T.Z. Harmathy, Ed., American Society or Testing and Materials, Philadelphia. Pp. 239–267.

Richardson, L. R. & Batista. 2000. M. Fire Resistance of Timber Decking for Heavy Timber Construction. Proc. International Conference on Fire Safety, Vol. 29. Pp. 33–45.

Schaffer, E. L. 1967. Charring rate of selected woods – transverse to grain. Madison, USA: Forest Products Laboratory. Research Paper FPL 69. 22 p.

Shoub, H. & Son, B. C. 1973. Fire Endurance Tests of Polywood on Steel Joist Floor Assemblies, With and Without Ceiling. Tests Number 492 and 497. Gaithersburg MD, USA: National Bureau of Standards. (NBSIR 73-141).

Son, B. C. 1973. Fire Endurance Tests of Unprotected Wood-Floor Constructions for Single-Family Residences. Gaithersburg MD, USA: National Bureau of Standards. (NBSIR 73-263).

Stanke, J. 1969. Die Feuerwiderstandsfähigkeit von belasten Holztützen. Mitteilungen der Deitschen Geshellshaft für Holzforschung, Heft Nr. 56. (In Germany)

Tillander, K. & Keski-Rahkonen, O. 2001. Rakennusten syttymistaajuudet PRONTO-tietokannasta 1996–1999 (Building ignition frequencies frome the PRONTO database 1996–1999). Espoo: VTT Tiedotteita 2119. 66 p. + app. 16 p. ISBN 951-38-5929-0; 951-38-5930-4. (In Finnish). http://www.vtt.fi/inf/pdf/tiedotteet/2001/T2119.pdf

Tillander, K. & Keski-Rahkonen, O. 2000. The influence of fire department intervention to the fire safety of a building assessed using fire risk analysis. Proceedings of the 3rd International Conference on Performance-Based Codes and Fire Safety Design Methods. Lund: 15–17 June 2000. Pp. 247–225.

Tillander, K. 2004. Utilisation of statistics to assess fire risks in buildings. Doctor's Thesis. Espoo: VTT Publications 537. 224 p. + app. 37 p. ISBN 951-38-6392-1; 951-38-6393-X. http://www.vtt.fi/inf/pdf/publications/2004/P537.pdf

Tinney, E.R. 1965. The combustion of wood dowels in heated air. 10th Symposium (International) on Combustion, The Combustion Institute. Pp. 925–930.

Toratti, T. & Turk, G. 2005. COST E24 Final Seminar, to be published.

Tran, H. C. & White, R. H. 1992. Burning rate of solid wood measured in a heat release rate calorimeter. Fire and materials, Vol. 16. Pp. 197–206.

Tsantaridis, L. D. & Östman, B. A. L. 1998. Charring of Protected Wood Studs. Fire and Materials, Vol. 22. Pp. 55–60.

White, R. H. & Tran, H. C. 1996. Charring Rate of Wood Exposed to a Constant Heat Flux. In: Wood and fire safety. Proceedings of the 3rd International Scientific Conference. The High Tatras, Slovak Republic, May 6–9. 9 p.

White, R. H. 2000. Charring Rate of Composite Timber Products. Wood and Fire Safety 2000, (Ed. Osvald, A). Proceedings of Wood & Fire Safety 2000 (part one). Nikara Krupina: Technical University of Zvolen. Pp. 353–363.

White, R. H., Schaffer, E. L. & Woeste, F. E. 1984. Replicate Fire Endurance Tests of an Unprotected Wood Joist Floor Assembly. Wood and Fiber Science, Vol. 16. Pp. 374–390.

VTT WORKING PAPERS

VTT RAKENNUS- JA YHDYSKUNTATEKNIIKKA –
VTT BYGG OCH TRANSPORT – VTT BUILDING AND TRANSPORT

4 Hietaniemi, Jukka, Hostikka, Simo & Vaari, Jukka. FDS simulation of fire spread – comparison of model results with experimental data. 2004. 46 p. + app. 6 p.

6 Viitanen, Hannu. Betonin ja siihen liittyvien materiaalien homehtumisen kriittiset olosuhteet – betonin homeenkesto. 2004. 25 s.

7 Gerlander, Riitta & Koivu, Tapio. Asiantuntijapalvelu yritysten innovaatiojohtamisen kehittämiseksi Piilaakson osaamiseen tukeutuen. IMIT SV -hankkeen loppuraportti. 2004. 25 s. + liitt. 11 s.

11 Lakka, Antti. Rakennustyömaan tuottavuus. 2004. 26 s. + liitt. 15 s.

14 Koivu, Tapio, Tukiainen, Sampo, Nummelin, Johanna, Atkin, Brian & Tainio, Risto. Institutional complexity affecting the outcomes of global projects. 2004. 59 p. + app. 2 p.

15 Rönty, Vesa, Keski-Rahkonen, Olavi & Hassinen, Jukka-Pekka. Reliability of sprinkler systems. Exploration and analysis of data from nuclear and non-nuclear installations. 2004. 89 p. + app. 9 p.

18 Nyyssönen, Teemu, Rajakko, Jaana & Keski-Rahkonen, Olavi. On the reliability of fire detection and alarm systems. Exploration and analysis of data from nuclear and non-nuclear installations. 2005. 62 p. + app. 6 p.

19 Tillander, Kati, Korhonen, Timo & Keski-Rahkonen, Olavi. Pelastustoimen määräiset seurantamittarit. 2005. 123 s. + liitt. 5 s.

20 Simo Hostikka & Johan Mangs. MASIFIRE – Map Based Simulation of Fires in Forest-Urban Interface. Reference and user's guide for version 1.0. 2005. 52 p. + app. 2 p.

21 Kortesmaa, Markku & Kevarinmäki, Ari. Massiivipuu maatilarakentamisessa. Suunnitteluohje. 2005. 76 s. + liitt. 6 s.

22 Ojanen, Tuomo & Ahonen, Jarkko. Moisture performance properties of exterior sheathing products made of spruce plywood or OSB. 2005. 52 p. + app. 12 p.

27 Kevarinmäki, Ari. Konenaulojen ulosvetolujuus. 2005. 24 s. + liitt. 12 s.

31 Hietaniemi, Jukka. A Probabilistic Approach to Wood Charring Rate. 2005. 53 p.

ISBN 951–38–6583–5 (URL: http://www.vtt.fi/inf/pdf/)
ISSN 1459–7683 (URL: http://www.vtt.fi/inf/pdf/)